Adaptive Tracking Control of Uncertain Switched Two-Time-Scale Systems With Full State Constraints

Meng-Ru Kong[a,b], Yan-Wu Wang[a,b,*], Irinel-Constantin Morărescu[c], Yan Lei[d]

a. School of Artificial Intelligence and Automation, Huazhong University of Science and Technology, Wuhan 430074, China

b. Key Laboratory of Image Processing and Intelligent Control, Ministry of Education, Huazhong University of Science and Technology, Wuhan 430074, China

c. CNRS, University of Lorraine, Nancy 54000, France

d. College of Electronic and Information Engineering, Southwest University, Chongqing 400715, China

Abstract—This paper investigates the tracking control problem for uncertain switched two-time-scale systems (TTSSs) subject to full state constraints (FSCs). In our design, instead of employing the commonly used barrier Lyapunov function (BLF), a unified framework is established by integrating a nonlinear transformed function (NTF) with a change of coordinates to address the FSCs, which can eliminate the feasibility conditions on the virtual controls. Moreover, this method can also handle the case of time-varying state constraints (SCs) and constraint-free cases without changing the structure of the controller. Based on a mode-dependent and ε-dependent Lyapunov function, a single-parameter-estimation-based control strategy is developed for the uncertain switched TTSSs, significantly reducing the design complexity. Finally, employing the improved admissible edge-dependent average dwell-time (AED-ADT) scheme in conjunction with Lyapunov techniques, it is ultimately verified that all signals in the closed-loop system are bounded, the tracking error converges to a bounded compact set, and the system states do not violate the given constraints.

Keywords—Switched two-time-scale systems, full state constraints, admissible edge-dependent average dwell-time, one parameter estimation.

1 Introduction

Switched systems are a specific class of hybrid systems, which are widely used in the modeling of many real systems [1–3]. For the stability analysis of switched systems, one can find popular methods based on state dependent switching but also methods based on time dependent switching, which generally require either a dwell-time (DT) or an average dwell-time (ADT), or a mode-dependent average dwell-time (MDADT). [4] investigates the recurrent stabilizability of discrete-time switched linear systems under switching constraints defined by a nondeterministic finite automaton, providing necessary and sufficient conditions and exploring its relation to control Lyapunov functions and initial states. Two stabilization strategies are proposed in [5] for continuous-time switched linear systems: an open-loop approach based on minimum DT using multiple Lyapunov functions, and a closed-loop method via Lyapunov–Metzler inequalities accounting for chattering. [6] shows

* Corresponding author. E-mail: wangyw@hust.edu.cn (Y.-W. Wang)

that ADT switching among stable systems ensures uniform exponential stability, and the results extend to certain nonlinear systems and hysteresis-based adaptive control. [7] demonstrates that a switched nonlinear system exhibits multiple practical input-to-state stable (ISS)-like characteristics under ADT switching signals, provided that every individual dynamical system within it is ISS. Furthermore, the concept of MDADT is built in [8] by extending the ADT method, which prevents the occurrence of sliding mode and has been extensively applied in the control design of switched systems [9–11]. In addition, adaptive tracking control under communication constraints and cyber attacks has attracted increasing attention. For instance, an adaptive event-triggered tracking strategy is developed in [12] for nonlinear networked systems subject to dynamic quantization and deception attacks. Meanwhile, to further relax the constraints on switching signals and enhance the stability conditions of slowly switched systems, the concept of admissible edge-dependent average dwell-time (AED-ADT) is presented in [13].

Many practical engineering systems involve dynamic processes evolving at significantly different time scales. For instance, in motor systems [14], electromagnetic transients are typically much faster than mechanical responses. Similar slow-fast characteristics can also arise in systems containing fast electrical dynamics and relatively slow mechanical dynamics. Meanwhile, changes in operating conditions, component configurations, or working modes may introduce switching behavior. Therefore, switched systems with slow-fast dynamics provide a useful framework for describing such engineering processes. Two-time-scale systems (TTSSs), also known as singularly perturbed systems, characterize the separation between fast and slow dynamics through a small singular perturbation parameter (SPP). This framework also provides useful tools for alleviating difficulties such as high dimensionality and ill conditioning that may arise when conventional single-time-scale methods are directly applied; see, e.g., [15–18]. When switching behavior is further involved, these systems are referred to as switched TTSSs [19–23]. Specifically, [19,20] investigate the stabilization problems for switched TTSSs subject to deception attacks by utilizing the ADT approach. The fuzzy control for discrete nonlinear switched TTSSs in finite time is studied in [21] by using the MDADT method. [22,23] address the problems for controller design and stability analysis of switched TTSSs with actuator saturation. However, these results ignore the constraints on the system states.

When deploying a control system in real applications, state constraints (SCs), static or dynamic, may be encountered. Violating these constraints can degrade system performance and may even lead to instability of the closed-loop system. Many current methods are well-established to handle state constraints, such as barrier Lyapunov function (BLF) methods [24–26], predictive control methods [27–29], and projected control methods [30, 31]. As discussed in [24–26], classical BLF-based constrained control schemes require explicit upper and lower bounds on virtual control laws to guarantee feasibility conditions. However, such bounds are generally difficult or impossible to compute analytically for uncertain switched TTSSs, especially when fast and slow dynamics are coupled. To completely remove these restrictive conditions, the studies in [32–34] propose novel methods based on nonlinear state-dependent functions to directly address the asymmetric full state constraints (FSCs). The methods are implemented for the traditional continuous time dynamics evolving on a

single time scale. Addressing the problem in the singularly perturbed setup is even more challenging. To this end, [35] further addresses the tracking control problem for nonlinear uncertain TTSSs with FSCs by using the approach in [32]. It is important to note that the results in [32–35] have to be carefully tackled in order to extend them to the case of switched systems. While switched TTSSs have been studied under ADT/MDADT/AED-ADT switching (e.g., [19–23]), these works neglect FSCs, and directly extending existing constrained control methods to switched TTSSs is nontrivial due to the interaction between switching, singular perturbations, and constraint enforcement. Moreover, existing constrained approaches [32, 33, 35] are specifically designed for constrained systems and fail to reduce to standard state feedback when constraints are removed. This limitation prevents seamless applicability across constrained, time-varying constrained, and constraint-free scenarios.

Meanwhile, parameter uncertainties and communication-induced effects such as quantization are also frequently encountered in practical control systems. For example, [36] investigates quantized fuzzy guaranteed cost control for electric-vehicle lateral dynamics with norm-bounded uncertain parameters. From a practical viewpoint, slow-fast dynamics, switching behavior, and state constraints may coexist in the same system. For example, physical variables such as speed, current, or other internal states are often required to remain within prescribed operating ranges for safety and reliable operation. Moreover, these allowable ranges may change with operating conditions or may not be imposed in some applications. It is therefore desirable to develop a control framework that can accommodate switching and different time scales while handling different forms of state constraints without redesigning the controller. This consideration provides the practical motivation for studying uncertain switched TTSSs under FSCs. Building on the preceding discussion, this paper investigates the tracking control problem for uncertain switched TTSSs with FSCs. The main challenges of the considered problem are twofold. First, the interaction among switching, slow-fast dynamics, and state constraints makes it difficult to directly extend existing constrained control methods to switched TTSSs. In particular, the feasibility conditions required by conventional BLF-based methods become difficult to verify when system uncertainties and slow-fast coupling are involved. Second, the presence of mode-dependent uncertainties increases the complexity of adaptive controller design, since multiple parameter updates may be required when conventional adaptive schemes are employed. These difficulties motivate the development of a simpler adaptive control strategy and a constraint-handling method without feasibility conditions for uncertain switched TTSSs. The primary innovations of this study are outlined below.

1. To reduce the complexity caused by parameter estimation in the adaptive design, a single-parameter-estimation-based control strategy is developed for uncertain switched TTSSs, where the adaptive law is independent of the switching mode. Compared with the existing result for uncertain TTSSs in [35], only one parameter update is required throughout the control design, which simplifies the design procedure and reduces the online computational burden.

2. To address the difficulty associated with the feasibility conditions in conventional BLF-based methods [24–26], a unified constraint-handling framework is established by combining the

nonlinear transformed function (NTF) with a modified change of coordinates. This framework eliminates the feasibility conditions on the virtual controls and can simultaneously handle symmetric/asymmetric, constant/time-varying, and constraint-free cases without changing the basic controller structure.

The structure of the paper is organized as follows: Section 2 introduces the problem formulation and necessary preliminaries. Section 3 presents the main theoretical results. Numerical simulations are provided in Section 4, followed by conclusion in Section 5.

2 Problem Formulation and Preliminaries

2.1 System Description

Consider the following uncertain switched TTSSs [35]:

$$\begin{cases} \dot{x}_1 = F_1^{\sigma(t)}(x_1, \theta_1) + G_1^{\sigma(t)}(x_1)x_2 \\ E(\varepsilon)\dot{x}_2 = F_2^{\sigma(t)}(x_1, x_2, \theta_2) + G_2^{\sigma(t)}(x_1, x_2)u \\ y = x_1 \end{cases} \tag{1}$$

where $x_1 = [x_{11}, x_{12}, \ldots, x_{1m}]^{\mathrm{T}} \in \mathbb{R}^m$ and $x_2 = [x_{21}, \ldots, x_{2m_1}, x_{2m_1+1}, \ldots, x_{2m}]^{\mathrm{T}} \in \mathbb{R}^m$ are the system states. The switching signal $\sigma(t) : [0, \infty) \to \Omega = \{1, 2, ..., M\}$ is a piecewise right-continuous constant function with $M \in \mathbb{N}$ being the number of modes. $u = [u_1, \ldots, u_m]^{\mathrm{T}} \in \mathbb{R}^m$ and $y \in \mathbb{R}^m$ are the control input vector and output vector of the system, respectively. $F_i^{\sigma(t)}(\cdot) \in \mathbb{R}^m$, $i = 1, 2$, denotes the uncertain nonlinear function vector including external disturbances or system modeling uncertainties, and $\theta_i \in \mathbb{R}^{r_i}$ is the unknown constant parameter vector inseparable from $F_i^{\sigma(t)}(\cdot)$. $G_i^{\sigma(t)}(\cdot) \in \mathbb{R}^{m\times m}$, $i = 1, 2$, is the unknown time-varying control coefficient matrix. ε is the SPP satisfying $0 < \varepsilon \ll 1$, and

$$E(\varepsilon) = \begin{bmatrix} I_{m_1\times m_1} & 0 \\ 0 & \varepsilon I_{m_2\times m_2} \end{bmatrix} \in \mathbb{R}^{m\times m}, \quad m_1 + m_2 = m.$$

In the following, the argument for a variable or function can be omitted if it is unlikely to cause confusion.

In system (1), x_1 and $\bar{x}_{2m_1} = [x_{21}, \ldots, x_{2m_1}]^{\mathrm{T}} \in \mathbb{R}^{m_1}$ are the slow state vectors, and $\bar{x}_{2m_2} = [x_{2m_1+1}, \ldots, x_{2m}]^{\mathrm{T}} \in \mathbb{R}^{m_2}$ is the fast state vector, which are required to satisfy the following asymmetric constraints:

$$x_{ik} \in \mathcal{D}_{ik} := \{x_{ik} \in \mathbb{R} | -\underline{D}_{ik} < x_{ik} < \overline{D}_{ik}\} \tag{2}$$

provided $-\underline{D}_{ik} < x_{ik}(0) < \overline{D}_{ik}$, $i = 1, 2$, $k = 1, \ldots, m$, where $\underline{D}_{ik}$ and $\overline{D}_{ik}$ are known positive constants, and $-\underline{D}_{ik}$ and $\overline{D}_{ik}$ specify the lower and upper constraint bounds of x_{ik}, respectively.

The control objectives of this work are:

P_1**:** A robust adaptive controller is constructed based on one parameter update for uncertain switched TTSSs with FSCs or constraint-free.

P_2**:** All signals in the closed-loop system are bounded and the tracking error $e = x_1 - y_d = [e_1, \ldots, e_m]^{\mathrm{T}} \in \mathbb{R}^m$, with $y_d = [y_{d1}, \ldots, y_{dm}]^{\mathrm{T}}$ being the known desired signal, converges to a small neighborhood of the origin.

P_3**:** The asymmetric FSCs (2) are maintained without imposing feasibility conditions on the virtual controls.

The analysis requires the following assumptions and a definition.

Assumption 1 [24] *The desired signal vectors y_d, $\dot{y}_d$, $\ddot{y}_d$ are available and continuous in known compact set $\mathcal{D}_d := \{[y_d^{\mathrm{T}}, \dot{y}_d^{\mathrm{T}}, \ddot{y}_d^{\mathrm{T}}]^{\mathrm{T}} | y_d^{\mathrm{T}} y_d + \dot{y}_d^{\mathrm{T}} \dot{y}_d + \ddot{y}_d^{\mathrm{T}} \ddot{y}_d \leq D_0\}$ with D_0 being a positive constant. Moreover, there exist positive constants $\overline{D}_{dk}$, $\underline{D}_{dk}$, $k = 1, \ldots, m$, satisfying $y_{dk} \in \mathcal{D}_{dk} := \{-\underline{D}_{1k} < -\underline{D}_{dk} \leq y_{dk} \leq \overline{D}_{dk} < \overline{D}_{1k}\}$.*

Assumption 2 [24] *There exist unknown positive constants $b_i^p, i = 1, 2, p \in \Omega$, and known non-negative smooth functions $\varphi_i^p(\bar{x}_i) : \mathbb{R}^{im} \to \mathbb{R}_+$ such that, for $x_{ik} \in \mathcal{D}_{ik}$, the uncertainties $F_i^p(\cdot)$ satisfy $\|F_i^p(\cdot)\| \leq b_i^p \varphi_i^p(\cdot)$, where $\bar{x}_1 = x_1$, $\bar{x}_2 = [x_1^{\mathrm{T}}, x_2^{\mathrm{T}}]^{\mathrm{T}}$. If $\bar{x}_i$ are bounded, so are F_i^p and φ_i^p.*

Assumption 3 [37] *The control coefficient matrices $G_i^p(\cdot), i = 1, 2, p \in \Omega$, are bounded and positive definite, namely, there exist positive constants $g_{i,m}^p$ and $g_{i,M}^p$ such that $x^{\mathrm{T}} G_i^p x \geq g_{i,m}^p x^{\mathrm{T}} x > 0$ for any $x \in \mathbb{R}^m \setminus \{0\}$, and $\|G_i^p\| \leq g_{i,M}^p$.*

Remark 1 *Assumption 1 regarding the desired signal y_d has been commonly used in the existing literature [24–26]. For Assumption 2, such a relationship may always be established by providing only basic information on $F_i^p(\bar{x}_i)$, $i = 1, 2, p \in \Omega$. Assumption 3 specifies the boundedness of the control gain matrices and reasonably requires that $G_i^p(\bar{x}_i)$, $i = 1, 2, p \in \Omega$, remains nonzero to ensure system controllability.*

Definition 1 [13] *For all pairs $(p, q) \in \Omega \times \Omega$, let $N_{p,q}^{\sigma}(t, T)$ denote the number of transitions from the qth subsystem to the pth subsystem within the interval $[t, T)$, and let $T_{p,q}(t, T)$ represent the total activation time of subsystem p over $[t, T)$, conditioned on such transitions occurring. The switching signal $\sigma(t)$ is said to satisfy an AED-ADT $\tau_{p,q}^a$ if there exist positive constants $\mathcal{N}_{p,q}^0$ and $\tau_{p,q}^a$ such that*

$$\mathcal{N}_{p,q}^{\sigma}(t, T) \leq \mathcal{N}_{p,q}^0 + \frac{T_{p,q}(t, T)}{\tau_{p,q}^a}, \quad \forall\, T \geq t \geq 0,$$

where $\mathcal{N}_{p,q}^0$ is referred to as the admissible edge-dependent chatter bound.

The primary motivation for introducing the AED-ADT technique stems from the intrinsic characteristics of switched TTSSs. In such systems, the interaction between slow and fast dynamics leads to mode-dependent transient behaviors, and different switching transitions may induce significantly different Lyapunov jumps. Consequently, imposing a uniform dwell-time constraint on all switching signals, as in classical ADT or MDADT schemes [6–11], can be overly conservative and may

unnecessarily restrict the admissible switching sequences. To address this issue, the AED-ADT framework assigns dwell-time constraints in an edge-dependent manner, that is, for each ordered switching pair $(q \to p)$. This allows the switching logic to account for the direction of mode transitions and the corresponding Lyapunov mismatch between subsystems. As a result, the stability conditions can be relaxed while still guaranteeing overall system stability.

2.2 System Transformation

To directly impose the asymmetric FSCs on state variables for system (1), a NTF ξ_{ik} purely based upon system state is designed as follows:

$$\xi_{ik} = \frac{\overline{D}_{ik}\underline{D}_{ik}x_{ik}}{(\overline{D}_{ik} - x_{ik})(\underline{D}_{ik} + x_{ik})} \tag{3}$$

with the initial condition $x_{ik}(0)$ satisfying $x_{ik} \in \mathcal{D}_{ik}$, $i = 1, 2$, and $k = 1, \ldots, m$. From (3), ξ_{ik} is a scalar function of x_{ik}, which is continuously differentiable on the interval $\mathcal{D}_{ik}$. Moreover, $\xi_{ik} \to \infty$ as x_{ik} approaches the boundary of $\mathcal{D}_{ik}$ for any initial condition $x_{ik} \in \mathcal{D}_{ik}$. Thus, if $\xi_{ik} \in \mathcal{L}_\infty$, $x_{ik} \in \mathcal{D}_{ik}$ can be ensured, i.e., FSCs (2) are not violated as long as ξ_{ik} are bounded. Therefore, satisfying the FSCs (2) means ensuring the boundedness of ξ_{ik}.

Remark 2 *The advantages of the NTF (3) lies in the following aspects:*

(i) Compared to BLF-based approaches, it imposes less stringent restrictions on initial system states by introducing a direct technique to handle FSCs rather than using the conservative method of converting original constraints into tracking error bounds [24–26].

(ii) A specific NTF in [32] is expressed as: $\xi_i = \frac{x_i}{(\overline{D}_i - x_i)(\underline{D}_i + x_i)}$, $i = 1, \cdots, m$. *It can be observed that for the constraint-free cases (i.e.,* $\overline{D}_i = \underline{D}_i \to \infty$*), the function simplifies to* $\lim_{\overline{D}_i = \underline{D}_i \to \infty} \xi_i = \frac{x_i}{(\overline{D}_i - x_i)(\underline{D}_i + x_i)} = 0$. *This result implies that the NTF proposed in [32] fails to handle both constrained and unconstrained scenarios in a unified manner. However, in our paper, for the constraint-free cases, we have* $\lim_{\overline{D}_{ik} = \underline{D}_{ik} \to \infty} \xi_{ik} = \lim_{\overline{D}_{ik} = \underline{D}_{ik} \to \infty} \frac{\overline{D}_{ik}\underline{D}_{ik}x_{ik}}{(\overline{D}_{ik} - x_{ik})(\underline{D}_{ik} + x_{ik})} = x_{ik}$. *This indicates that the NTF* ξ_{ik} *reduces to the system state* x_{ik}*, enabling the function (3) to handle SCs or constraint-free cases of the system (1) in a unified manner without changing the controller structure. In fact, time-varying asymmetric SCs can also be solved by the proposed NTF, which will be discussed in Section 3.*

To facilitate the controller design, we define $\rho_{ik} = \frac{(\overline{D}_{ik} - x_{ik})(\underline{D}_{ik} + x_{ik})}{\overline{D}_{ik}\underline{D}_{ik}}$ and $\rho_i = \mathrm{diag}\{\rho_{i1}, \ldots, \rho_{im}\}$, for $i = 1, 2$, and $k = 1, \ldots, m$. With this notation, one gets

$$x_i = \rho_i \xi_i \tag{4}$$

with $\xi_i = [\xi_{i1}, \ldots, \xi_{im}]^{\mathrm{T}}$. Then the derivative of ξ_{ik} in (3) is obtained as:

$$\dot{\xi}_{ik} = \lambda_{ik}\dot{x}_{ik}, \tag{5}$$

where $\lambda_{ik} = \frac{\overline{D}_{ik}\underline{D}_{ik}(\overline{D}_{ik}\underline{D}_{ik}+x_{ik}^2)}{(\overline{D}_{ik}-x_{ik})^2(\underline{D}_{ik}+x_{ik})^2}$, $i = 1, 2$, and $k = 1, \ldots, m$, is well defined in set $\mathcal{D}_{ik}$. Combining (1) and (4), we can rewrite (5) as

$$\begin{cases} \dot{\xi}_1 = \lambda_1(F_1^{\sigma(t)} + G_1^{\sigma(t)}\rho_2\xi_2) \\ E(\varepsilon)\dot{\xi}_2 = \lambda_2(F_2^{\sigma(t)} + G_2^{\sigma(t)}u) \end{cases} \tag{6}$$

with $\lambda_i = \mathrm{diag}\{\lambda_{i1}, \ldots, \lambda_{im}\}$ being a positive definite diagonal matrix when $x_{ik} \in \mathcal{D}_{ik}$, $i = 1, 2$, and $k = 1, \ldots, m$.

3 Main Results

3.1 Single-Parameter-Estimation-Based Controller Design

In this section, the dynamic surface control (DSC) method is utilized to construct a robust adaptive controller based on one parameter estimation for system (1) with FSCs, in which the feasibility conditions in [24–26] can be entirely eliminated. As an essential step in the control design, the conventional change of coordinates $z_1 = x_1 - y_d$ in [25] is no longer directly applicable due to the introduction of the NTF (3). Instead, a modified change of coordinates tailored to the structure of the NTF (3) is developed to facilitate the subsequent design of the virtual control law α_1. To this end, we introduce the following change of coordinates:

$$\begin{cases} z_1 = \xi_1 - \alpha_{1f} \\ z_2 = \xi_2 - \alpha_{2f} \end{cases} \tag{7}$$

where z_i, $i = 1, 2$, is the virtual error, ξ_i is introduced to handle FSCs without imposing the feasibility conditions on virtual control laws, $\alpha_{1f} = [\alpha_{1f,1}, \ldots, \alpha_{1f,m}]^{\mathrm{T}}$, $\alpha_{1f,k} = \frac{\overline{D}_{1k}\underline{D}_{1k}y_{dk}}{(\overline{D}_{1k}-y_{dk})(\underline{D}_{1k}+y_{dk})}$, $k = 1, \ldots, m$, and α_{2f} is obtained from the following first-order filter:

$$\kappa_2\dot{\alpha}_{2f} + \alpha_{2f} = \rho_2^{-1}\alpha_1, \tag{8}$$

where $\kappa_2 > 0$ is a design parameter, α_1 is a virtual controller designed later in (19), and ρ_2 is defined in (4). Then it can be seen from Assumption 1 that α_{1f} is calculable and bounded in the compact set $\mathcal{D}_d$. In order to facilitate the subsequent controller design and stability analysis, define the following filter error:

$$y_2 = \alpha_{2f} - \rho_2^{-1}\alpha_1. \tag{9}$$

Thus, according to (7) and (9),

$$\xi_2 = z_2 + \alpha_{2f} = z_2 + y_2 + \rho_2^{-1}\alpha_1. \tag{10}$$

Remark 3 *In conventional BLF methods (e.g., [24–26]), feasibility conditions require the virtual control signals to remain strictly within predefined bounds to prevent singularity of the BLF. This*

inevitably introduces parameter-dependent inequalities that must be verified a priori, which is extremely difficult for uncertain switched TTSSs due to the coupling between slow-fast dynamics and switching.

In contrast, our method removes this requirement through two key mechanisms:

(i) As defined in (3), the NTF maps each constrained state $x_{ik} \in \mathcal{D}_{ik}$ to an unconstrained variable $\xi_{ik} \in \mathbb{R}$, $i = 1, 2$, $k = 1, \ldots, m$. Importantly, constraint satisfaction is equivalently guaranteed by the boundedness of ξ_{ik}, rather than by bounding the virtual controls.

(ii) Instead of the traditional virtual errors $z_i = x_i - \alpha_{i-1}$ in [25], the modified forms $z_i = \xi_i - \alpha_{if}$ in (7) ensure that the virtual errors are defined entirely in the transformed space. As a result, the stability analysis only requires the boundedness of z_i and ξ_i, without imposing any explicit upper or lower bounds on the virtual control α_1.

The detailed process of the adaptive backstepping control based on one parameter update is given as follows.

Step 1: For $p \in \Omega$, taking the derivative of $z_1 = \xi_1 - \alpha_{1f}$ along (6), we can obtain from (10)

$$\dot{z}_1 = \dot{\xi}_1 - \dot{\alpha}_{1f} = \lambda_1(F_1^p + G_1^p\rho_2\xi_2) - \dot{\alpha}_{1f} = \lambda_1(F_1^p + G_1^p\rho_2(z_2 + y_2) + G_1^p\alpha_1) - \dot{\alpha}_{1f} \tag{11}$$

with $\dot{\alpha}_{1f} = \lambda_d\dot{y}_d$, $\lambda_d = \mathrm{diag}\{\lambda_{d1}, \ldots, \lambda_{dm}\}$, $\lambda_{dk} = \frac{\overline{D}_{1k}\underline{D}_{1k}(\overline{D}_{1k}\underline{D}_{1k}+y_{dk}^2)}{(\overline{D}_{1k}-y_{dk})^2(\underline{D}_{1k}+y_{dk})^2}$, $k = 1, \ldots, m$. From the definition of λ_{dk}, λ_d is positive definite and calculable in the compact sets $\mathcal{D}_{dk}$.

Choose a Lyapunov function candidate

$$V_1^p = \frac{1}{2g_{1,m}^p}z_1^{\mathrm{T}}z_1 + \frac{1}{2\gamma}\widetilde{\Theta}^2 + \frac{1}{2}y_2^{\mathrm{T}}y_2, \tag{12}$$

where $g_{1,m}^p$ is defined in Assumption 3, $\gamma > 0$ is a design parameter, $\widetilde{\Theta} = \Theta - \widehat{\Theta}$ is the parameter estimate error with $\widehat{\Theta}$ being the parameter estimate of $\Theta = \max\{(b_i^p)^2, 1\}$, $i = 1, 2, p \in \Omega$. Then the derivative of V_1^p along (12) yields

$$\dot{V}_1^p = \frac{1}{g_{1,m}^p}z_1^{\mathrm{T}}\left(\lambda_1F_1^p + \lambda_1G_1^p\rho_2z_2 + \lambda_1G_1^p\rho_2y_2 + \lambda_1G_1^p\alpha_1 - \dot{\alpha}_{1f}\right) - \frac{1}{\gamma}\widetilde{\Theta}\dot{\widehat{\Theta}} + y_2^{\mathrm{T}}\dot{y}_2. \tag{13}$$

By using Assumptions 1-3 and Young's inequality, we have

$$\frac{1}{g_{1,m}^p}z_1^{\mathrm{T}}\lambda_1F_1^p \le \frac{\|z_1\|^2\|\lambda_1\|^2\Theta\varphi_1}{2a^2} + \frac{a^2}{2(g_{1,\min})^2}, \tag{14}$$

$$-\frac{1}{g_{1,m}^p}z_1^{\mathrm{T}}\dot{\alpha}_{1f} \le \frac{\|z_1\|^2\|\lambda_d\dot{y}_d\|^2}{2a^2} + \frac{a^2}{2(g_{1,\min})^2}, \tag{15}$$

$$\frac{1}{g_{1,m}^p}z_1^{\mathrm{T}}\lambda_1G_1^p\rho_2y_2 \le \frac{(g_{1,\max})^2}{2a^2(g_{1,\min})^2}\|z_1\|^2\|\lambda_1\|^2 + \frac{a^2}{2}\|\rho_2\|^2\|y_2\|^2, \tag{16}$$

$$\frac{1}{g_{1,m}^p}z_1^{\mathrm{T}}\lambda_1G_1^p\rho_2z_2 \le \frac{1}{2a^2g_{2,m}^p}\|z_1\|^2\|\lambda_1\|^2\|\rho_2\|^2\|z_2\|^2 + \frac{a^2(g_{1,\max})^2g_{2,\max}}{2(g_{1,\min})^2}, \tag{17}$$

where $a > 0$ is a design parameter, $g_{1,\min} = \min_{p\in\Omega}\{g^p_{1,m}\}$, $g_{1,\max} = \max_{p\in\Omega}\{g^p_{1,M}\}$, $g_{2,\max} = \max_{p\in\Omega}\{g^p_{2,m}\}$, $\|\varphi^p_1\|^2 \le \varphi_1$, $p \in \Omega$. Substituting (14)-(17) into (13), we obtain

$$\begin{aligned}\dot{V}^p_1 \le & \Theta\Psi_1\|z_1\|^2 + \frac{1}{g^p_{1,m}} z_1^{\mathrm{T}}\lambda_1 G^p_1\alpha_1 + \frac{a^2}{2}\|\rho_2\|^2\|y_2\|^2 + \frac{1}{2a^2 g^p_{2,m}}\|z_1\|^2\|\lambda_1\|^2\|\rho_2\|^2\|z_2\|^2 \\ & - \frac{1}{\gamma}\widetilde{\Theta}\dot{\widehat{\Theta}} + y_2^{\mathrm{T}}\dot{y}_2 + \Lambda_1, \end{aligned} \tag{18}$$

where $\Psi_1 = \frac{1}{2a^2}\left(\|\lambda_1\|^2\varphi_1 + \|\lambda_d\dot{y}_d\|^2 + \frac{(g_{1,\max})^2}{(g_{1,\min})^2}\|\lambda_1\|^2\right)$ is a known and calculable scalar function, $\Lambda_1 = \frac{a^2}{(g_{1,\min})^2} + \frac{a^2(g_{1,\max})^2 g_{2,\max}}{2(g_{1,\min})^2}$ is a positive constant.

Let the virtual control α_1 be

$$\alpha_1 = -(c_1 + \widehat{\Theta}\Psi_1)(\lambda^*_1)^{-2}\lambda_1 z_1 \tag{19}$$

with $c_1 > 0$ being a design parameter, $\lambda^*_1 = \min\{\lambda^*_{1k}\}$, $\lambda^*_{1k} = \frac{16\overline{D}^2_{1k}\underline{D}^2_{1k}}{(\overline{D}_{1k}+\underline{D}_{1k})^4}$, $k = 1, \cdots, m$. Due to $\lambda_{1k} = \frac{\overline{D}_{1k}\underline{D}_{1k}(\overline{D}_{1k}\underline{D}_{1k}+x^2_{1k})}{(\overline{D}_{1k}-x_{1k})^2(\underline{D}_{1k}+x_{1k})^2} \ge \lambda^*_{1k}$ in $\mathcal{D}_{1k}$, then $z_1^{\mathrm{T}}\lambda_1 G^p_1\lambda_1 z_1 \ge g^p_{1,m}\sum_{k=1}^n(\lambda^*_{1k})^2 z^2_{1k} \ge g^p_{1,m}(\lambda^*_1)^2\|z_1\|^2$. Then inserting the virtual control law α_1 (19) into $\frac{1}{g^p_{1,m}} z_1^{\mathrm{T}}\lambda_1 G^p_1\alpha_1$, we have

$$\frac{1}{g^p_{1,m}} z_1^{\mathrm{T}}\lambda_1 G^p_1\alpha_1 = -\frac{(c_1 + \widehat{\Theta}\Psi_1)}{g^p_{1,m}}(\lambda^*_1)^{-2} z_1^{\mathrm{T}}\lambda_1 G^p_1\lambda_1 z_1 \le -(c_1 + \widehat{\Theta}\Psi_1)\|z_1\|^2. \tag{20}$$

Since (18) contains a nonlinear term $\frac{1}{g^p_{1,m}} z_1^{\mathrm{T}}\lambda_1 G^p_1\alpha_1$ and λ_1 is related to the NTF (3), it is necessary to use $(\lambda^*_1)^{-2}\lambda^2_1 \le -I$ to eliminate λ_1 of this nonlinear term in the process of designing α_1, thereby obtaining the result (20). Similar challenges will also arise in the design process of the controller (33). Consequently, combining (18) with (20), it follows that

$$\begin{aligned}\dot{V}^p_1 \le & -c_1\|z_1\|^2 + \widetilde{\Theta}\Psi_1\|z_1\|^2 - \frac{1}{\gamma}\widetilde{\Theta}\dot{\widehat{\Theta}} + y_2^{\mathrm{T}}\dot{y}_2 + \Lambda_1 \\ & + \frac{a^2}{2}\|\rho_2\|^2\|y_2\|^2 + \frac{1}{2a^2 g^p_{2,m}}\|z_1\|^2\|\lambda_1\|^2\|\rho_2\|^2\|z_2\|^2. \end{aligned} \tag{21}$$

Furthermore, according to the first-order filter in (8) and the filter error y_2 in (9), we have $\dot{y}_2 = \dot{\alpha}_{2f} - \frac{\mathrm{d}}{\mathrm{d}t}\left(\rho_2^{-1}\alpha_1\right) = -\frac{y_2}{\kappa_2} + \Upsilon(\cdot)$, where $\Upsilon\left(z_1, z_2, y_2, \widehat{\Theta}, y_d, \dot{y}_d, \ddot{y}_d\right) = -\frac{\mathrm{d}}{\mathrm{d}t}\left(\rho_2^{-1}\alpha_1\right) = -(\rho_2^{-1})'\alpha_1 - \rho_2^{-1}\left(\frac{\partial\alpha_1}{\partial\widehat{\Theta}}\dot{\widehat{\Theta}} + \frac{\partial\alpha_1}{\partial\Psi_1}\dot{\Psi}_1 + \frac{\partial\alpha_1}{\partial\lambda^*_1}\dot{\lambda}^*_1 + \frac{\partial\alpha_1}{\partial\lambda_1}\dot{\lambda}_1 + \frac{\partial\alpha_1}{\partial z_1}\dot{z}_1\right)$ is a continuous function in regions $\mathcal{D}_{ik}$ and $\dot{\widehat{\Theta}}$ will be given latter, $i = 1, 2$, and $k = 1, \ldots, m$. Therefore,

$$y_2^{\mathrm{T}}\dot{y}_2 = -\frac{y_2^{\mathrm{T}}y_2}{\kappa_2} + y_2^{\mathrm{T}}\Upsilon \le \left(\frac{1}{4} - \frac{1}{\kappa_2}\right)\|y_2\|^2 + \|\Upsilon\|^2. \tag{22}$$

Then, (21) can be rewritten as

$$\begin{aligned}\dot{V}^p_1 \le & -c_1\|z_1\|^2 + \widetilde{\Theta}\left(\Psi_1\|z_1\|^2 - \frac{1}{\gamma}\dot{\widehat{\Theta}}\right) + \frac{1}{2a^2 g^p_{2,m}}\|z_1\|^2\|\lambda_1\|^2\|\rho_2\|^2\|z_2\|^2 + \|\Upsilon\|^2 \\ & + \left(\frac{1}{4} + \frac{a^2}{2}\|\rho_2\|^2 - \frac{1}{\kappa_2}\right)\|y_2\|^2 + \Lambda_1. \end{aligned} \tag{23}$$

Choose a suitable constant $\bar{\kappa}_2 > 0$ such that $\frac{1}{\kappa_2} \geq \frac{1}{4} + \frac{a^2}{2}\|\rho_2\|^2 + \bar{\kappa}_2$. Hence, (23) can be further expressed as

$$\begin{aligned}\dot{V}_1^p \leq & -c_1\|z_1\|^2 + \widetilde{\Theta}\left(\Psi_1\|z_1\|^2 - \frac{1}{\gamma}\dot{\widehat{\Theta}}\right) - \bar{\kappa}_2\|y_2\|^2 \\ & + \frac{1}{2a^2 g_{2,m}^p}\|z_1\|^2\|\lambda_1\|^2\|\rho_2\|^2\|z_2\|^2 + \|\Upsilon\|^2 + \Lambda_1,\end{aligned} \tag{24}$$

where $\dot{\widehat{\Theta}}$ will be given in the next step.

Remark 4 *As shown in (19), the virtual control α_1 is a nonlinear function that relies on design parameters c_1, $\widehat{\Theta}$, and functions z_1, λ_1^*, λ_1, and Ψ_1. When employing the conventional BLF approaches [24–26] for control design, it is essential to explicitly determine both the upper and lower bounds of the virtual control α_1 to validate the feasibility conditions at this step. However, due to the absence of an explicit analytical solution for deriving these bounds, the verification of parameter existence requires the utilization of offline optimization techniques, which would substantially escalate the computational load. Furthermore, within a specified constrained domain, the identification of optimal parameters that satisfy the feasibility conditions may prove unattainable, thereby rendering BLF-based control algorithm ineffective in practical implementation. In this paper, a notable advantage lies in its elimination of the requirement to determine explicit bounds for the virtual controller α_1 since no feasibility conditions are required. This significant simplification is achieved through the NTF (3) and the change of coordinates (7), which enable stability analysis to be conducted solely based on the boundedness property of α_1.*

Step 2: Taking the derivative of $z_2 = \xi_2 - \alpha_{2f}$ along (6), for $p \in \Omega$, we have

$$E(\varepsilon)\dot{z}_2 = \lambda_2(F_2^p + G_2^p u) - E(\varepsilon)\dot{\alpha}_{2f}, \tag{25}$$

where $\dot{\alpha}_{2f}$ is well defined in (8).

Define a Lyapunov function candidate V_2^p as

$$V_2^p = \frac{1}{2g_{2,m}^p} z_2^{\mathrm{T}} E(\varepsilon) P z_2, \tag{26}$$

where $g_{2,m}^p$ is defined in Assumption 3, $P = \begin{bmatrix} P_{11} & 0 \\ 0 & P_{22} \end{bmatrix}$ with $P_{11} = P_{11}^{\mathrm{T}} > 0, P_{22} = P_{22}^{\mathrm{T}} > 0$, then $P = P^{\mathrm{T}} > 0$ and $E(\varepsilon)P = P^{\mathrm{T}}E(\varepsilon) > 0$. Employing (25) and (26), the derivative of V_2^p can be formulated as

$$\dot{V}_2^p = \frac{1}{g_{2,m}^p} z_2^{\mathrm{T}} P\left(\lambda_2 F_2^p + \lambda_2 G_2^p u - E(\varepsilon)\dot{\alpha}_{2f}\right). \tag{27}$$

Similar to (14)-(17), utilizing Assumptions 1-3 and Young's inequality gives

$$\frac{1}{g_{2,m}^p} z_2^{\mathrm{T}} P\lambda_2 F_2^p \leq \frac{\|z_2\|^2\|P\|^2\|\lambda_2\|^2\Theta\varphi_2}{2a^2 g_{2,m}^p} + \frac{a^2}{2g_{2,\min}}, \tag{28}$$

$$-\frac{1}{g_{2,m}^p} z_2^{\mathrm{T}} P E(\varepsilon)\dot{\alpha}_{2f} \leq \frac{\|z_2\|^2\|P\|^2\|E(\varepsilon)\dot{\alpha}_{2f}\|^2}{2a^2 g_{2,m}^p} + \frac{a^2}{2g_{2,\min}}, \tag{29}$$

where $\|\varphi_2^p\|^2 \leq \varphi_2$, $p \in \Omega$. Then substituting (28), (29) into (27), we have

$$\dot{V}_2^p \leq \frac{\|z_2\|^2\|P\|^2\|\lambda_2\|^2\Theta\varphi_2}{2a^2 g_{2,m}^p} + \frac{\|z_2\|^2\|P\|^2\|E(\varepsilon)\dot{\alpha}_{2f}\|^2}{2a^2 g_{2,m}^p} + \frac{1}{g_{2,m}^p} z_2^{\mathrm{T}} P\lambda_2 G_2^p u + \Lambda_2, \tag{30}$$

with $\Lambda_2 = \frac{a^2}{g_{2,\min}}$ being a positive constant.

Selecting the Lyapunov function candidate

$$V^p = V_1^p + V_2^p = \frac{1}{2g_{1,m}^p} z_1^{\mathrm{T}} z_1 + \frac{1}{2g_{2,m}^p} z_2^{\mathrm{T}} E(\varepsilon) P z_2 + \frac{1}{2\gamma}\widetilde{\Theta}^2 + \frac{1}{2} y_2^{\mathrm{T}} y_2, \tag{31}$$

and combining (24), (30) with (31), for the pth subsystem, we can infer that

$$\begin{aligned}\dot{V}^p \leq & -c_1\|z_1\|^2 - \bar{\kappa}_2\|y_2\|^2 + \widetilde{\Theta}\left(\Psi_1\|z_1\|^2 - \frac{1}{\gamma}\dot{\widehat{\Theta}}\right) + \|\Upsilon\|^2 + \Lambda \\ & + \frac{\Theta}{g_{2,m}^p}\Psi_2\|z_2\|^2 + \frac{1}{g_{2,m}^p} z_2^{\mathrm{T}} P\lambda_2 G_2^p u,\end{aligned} \tag{32}$$

where $\Lambda = \Lambda_1 + \Lambda_2$ and $\Psi_2 = \frac{1}{2a^2}\left(\|P\|^2\|\lambda_2\|^2\varphi_2 + \|P\|^2\|E(\varepsilon)\dot{\alpha}_{2f}\|^2 + \|z_1\|^2\|\lambda_1\|^2\|\rho_2\|^2\right)$.

Let the actual control law u and the adaptive law $\widehat{\Theta}$ be designed as

$$u = -\left(c_2 + \frac{\widehat{\Theta}}{g_{2,m}^p}\Psi_2\right)(\lambda_2^*)^{-2}\bar{\lambda}_P^{-1}\lambda_2 P z_2, \tag{33}$$

$$\dot{\widehat{\Theta}} = \gamma\left(\Psi_1\|z_1\|^2 + \frac{1}{g_{2,\min}}\Psi_2\|z_2\|^2\right) - l\widehat{\Theta}, \tag{34}$$

where c_2 and l are positive parameters, $\lambda_2^* = \min\{\lambda_{2k}^*\}$, $\lambda_{2k}^* = \frac{16\overline{D}_{2k}^2\underline{D}_{2k}^2}{(\overline{D}_{2k}+\underline{D}_{2k})^4}$, $k = 1, \cdots, m$, $\bar{\lambda}_P = \lambda_{\min}(P^2)$. $\widehat{\Theta}(0) \geq 0$ is an arbitrarily chosen initial estimate of $\widehat{\Theta}$. Noting that as $\gamma\left(\Psi_1\|z_1\|^2 + \frac{1}{g_{2,\min}}\Psi_2\|z_2\|^2\right) \geq 0$, it holds that $\widehat{\Theta}(t) \geq 0$ for any $\widehat{\Theta}(0) \geq 0$, $t \geq 0$. Due to $\lambda_{2k} = \frac{\overline{D}_{2k}\underline{D}_{2k}(\overline{D}_{2k}\underline{D}_{2k}+x_{2k}^2)}{(\overline{D}_{2k}-x_{2k})^2(\underline{D}_{2k}+x_{2k})^2} \geq \lambda_{2k}^*$ in $\mathcal{D}_{2k}$, $z_2^{\mathrm{T}} P\lambda_2 G_2^p\lambda_2 P z_2 \geq g_{2,m}^p(\lambda_2^*)^2\bar{\lambda}_P\|z_2\|^2$ and $\frac{1}{g_{2,m}^p} z_2^{\mathrm{T}} P\lambda_2 G_2^p u \leq -(c_2 + \frac{\widehat{\Theta}}{g_{2,m}^p}\Psi_2)\|z_2\|^2$. Thus, substituting the actual control law u (33) and the adaptive law $\dot{\widehat{\Theta}}$ (34) into (32), and utilizing the fact that $\frac{l}{\gamma}\widetilde{\Theta}\widehat{\Theta} \leq -\frac{l}{2\gamma}\widetilde{\Theta}^2 + \frac{l}{2\gamma}\Theta^2$, we have

$$\dot{V}^p \leq -c_1\|z_1\|^2 - c_2\|z_2\|^2 - \bar{\kappa}_2\|y_2\|^2 - \frac{l}{2\gamma}\widetilde{\Theta}^2 + \|\Upsilon\|^2 + K_1 \tag{35}$$

with $K_1 = \Lambda + \frac{l}{2\gamma}\Theta^2$.

Remark 5 *In the majority of existing adaptive control algorithms for state-constrained nonlinear systems [32, 35], an adaptive law is required to estimate an unknown constant parameter or an unknown parameter vector at every step of the backstepping procedure. As the system order increases, this process becomes computationally demanding due to the need for multiple parameter estimations and the increasing complexity of the control design. To address this issue, utilizing the norm estimation approach [38], only a single parameter estimation is performed throughout the control process, which significantly reduces the overall computational burden.*

In order to facilitate subsequent stability analysis, define the following positive constants:

$$\mu_p < \min\{2c_1 g_{1,m}^p, \frac{2c_2 g_{2,m}^p}{\lambda_{\max}\{E(\varepsilon)P\}}, 2\bar{\kappa}_2, l\}, \tag{36}$$

$$\hbar_{p,q} > \max\left\{\frac{g_{1,m}^q}{g_{1,m}^p}, \frac{g_{2,m}^q}{g_{2,m}^p}, 1\right\}, \tag{37}$$

$$K = K_1 + K_2^2, \tag{38}$$

where $p, q \in \Omega$, and K_2 will be defined later.

3.2 Stability Analysis

Theorem 1 *Consider the uncertain switched TTSSs (1) with asymmetric FSCs under the controller (33) and the adaptive law (34). Let the Lyapunov function candidate be designed as (31). If $x_{ik}(0) \in \mathcal{D}_{ik}$, $i = 1, 2$, and $k = 1, \ldots, m$, the AED-ADT of the switching signal $\sigma(t)$ satisfies $\tau_{p,q}^a > \frac{\ln \hbar_{p,q}}{\mu_p}$, and there exists a positive constant B_0 such that $V^p(0) \leq B_0$, $p \in \Omega$, then under Assumptions 1-3, the control objectives P_1-P_3 can be achieved through the single-parameter-estimation-based adaptive control.*

Proof: Let the sets $\mathcal{D}_d := \left\{[y_d^{\mathrm{T}}, \dot{y}_d^{\mathrm{T}}, \ddot{y}_d^{\mathrm{T}}]^{\mathrm{T}} | y_d^{\mathrm{T}} y_d + \dot{y}_d^{\mathrm{T}} \dot{y}_d + \ddot{y}_d^{\mathrm{T}} \ddot{y}_d \leq D_0\right\} \subset \mathbb{R}^{3m}$, $\mathcal{D}_{V^p} := \Big\{[z_1^{\mathrm{T}}, z_2^{\mathrm{T}}, \widetilde{\Theta}, y_2^{\mathrm{T}}]^{\mathrm{T}} | \frac{1}{g_{1,m}^p} z_1^{\mathrm{T}} z_1 + y_2^{\mathrm{T}} y_2 + \frac{1}{g_{2,m}^p} z_2^{\mathrm{T}} E(\varepsilon) P z_2 + \frac{1}{\gamma}\widetilde{\Theta}^2 \leq 2B_0\Big\} \subset \mathbb{R}^{3m+1}$, then $\mathcal{D}_d \times \mathcal{D}_{V^p}$ is a compact set and there exists a constant $K_2 > 0$ such that $\|\Upsilon\| \leq K_2$ on $\mathcal{D}_d \times \mathcal{D}_{V^p}$, where Υ is given in (22). For the pth subsystem, it follows from (35) that

$$\dot{V}^p \leq -c_1\|z_1\|^2 - c_2\|z_2\|^2 - \bar{\kappa}_2\|y_2\|^2 - \frac{l}{2\gamma}\widetilde{\Theta}^2 + K_1 + K_2^2 \leq -\mu_p V^p + K, \tag{39}$$

and $\forall(\sigma(t_k) = p, \sigma(t_k^-) = q) \in \Omega \times \Omega$, $p \neq q$,

$$V^p \leq \hbar_{p,q} V^q. \tag{40}$$

For an arbitrary $T > 0$, let $t_0 = 0$ and $t_1, t_2, \ldots, t_k, t_{k+1}, \ldots, t_{\mathcal{N}^\sigma(0,T)}$ denote the switching instants on the interval $[0, T]$, in which $\mathcal{N}^\sigma(0,T) = \sum_{p=1}^M \mathcal{N}_p^\sigma(0,T)$ and $\mathcal{N}_p^\sigma(0,T) = \sum_{q=1, p\neq q}^M \mathcal{N}_{p,q}^\sigma(0,T)$, where $\mathcal{N}^\sigma(0,T)$ is the switching number of $\sigma(t)$ and $\mathcal{N}_p^\sigma(0,T)$ is the switching number when the pth subsystem is activated during the interval $[0, T]$, $p \in \Omega$.

Let $\Xi(t) = e^{\mu_{\sigma(t)}t} V^{\sigma(t)}(Z(t))$ with $Z(t) = [z_1^{\mathrm{T}}, z_2^{\mathrm{T}}, y_2^{\mathrm{T}}, \widetilde{\Theta}]^{\mathrm{T}}$ being piecewise differentiable along solutions of the system. On each interval $[t_k, t_{k+1})$, using (39), it can be inferred that

$$\dot{\Xi}(t) \leq \mu_{\sigma(t)} e^{\mu_{\sigma(t)}t} V^{\sigma(t)}(Z(t)) + K e^{\mu_{\sigma(t)}t} - \mu_{\sigma(t)} e^{\mu_{\sigma(t)}t} V^{\sigma(t)}(Z(t)) = K e^{\mu_{\sigma(t)}t}, \tag{41}$$

which implies

$$\int_{t_k}^{t_{k+1}} \dot{\Xi}(t)\mathrm{d}t = \Xi(t_{k+1}) - \Xi(t_k) \leq \int_{t_k}^{t_{k+1}} K e^{\mu_{\sigma(t)}t}\mathrm{d}t. \tag{42}$$

Employing (40)-(42), we have

$$\begin{aligned}\Xi(t_{k+1}) &\leq \hbar_{\sigma(t_{k+1}),\sigma(t_{k+1}^-)} e^{\left(\mu_{\sigma(t_{k+1})}-\mu_{\sigma(t_{k+1}^-)}\right)t_{k+1}}\Xi(t_{k+1}^-)\\ &\leq \Gamma_{1,k}\Xi(t_k)+\Gamma_{1,k}\int_{t_k}^{t_{k+1}} Ke^{\mu_{\sigma(t_k)}t}\mathrm{d}t\\ &\leq \Gamma_{1,k-1}\Xi(t_{k-1})+\Gamma_{1,k-1}\int_{t_{k-1}}^{t_k} Ke^{\mu_{\sigma(t_{k-1})}t}\mathrm{d}t+\Gamma_{1,k}\int_{t_k}^{t_{k+1}} Ke^{\mu_{\sigma(t_k)}t}\mathrm{d}t\\ &\ \ \vdots\\ &\leq \prod_{l=0}^{k}\hbar_{\sigma(t_{l+1}),\sigma(t_l)} e^{\sum_{l=0}^{k}\left(\mu_{\sigma(t_{l+1})}-\mu_{\sigma(t_l)}\right)t_{l+1}}\Xi(t_0)+\sum_{l=0}^{k}\Gamma_{1,l}\int_{t_l}^{t_{l+1}} Ke^{\mu_{\sigma(t_l)}t}\mathrm{d}t. \end{aligned} \tag{43}$$

where $\Gamma_{1,k}=\hbar_{\sigma(t_{k+1}),\sigma(t_k)}\exp\left\{(\mu_{\sigma(t_{k+1})}-\mu_{\sigma(t_k)})t_{k+1}\right\}$, $\Gamma_{1,k-1}=\hbar_{\sigma(t_{k+1}),\sigma(t_k)}\hbar_{\sigma(t_k),\sigma(t_{k-1})}\times\exp\left\{(\mu_{\sigma(t_{k+1})}-\mu_{\sigma(t_k)})t_{k+1}+(\mu_{\sigma(t_k)}-\mu_{\sigma(t_{k-1})})t_k\right\}$, $\Gamma_{1,l}=\prod_{s=l}^{k}\hbar_{\sigma(t_{s+1}),\sigma(t_s)}\exp\left\{\sum_{s=l}^{k}(\mu_{\sigma(t_{s+1})}-\mu_{\sigma(t_s)})t_{s+1}\right\}$.

Furthermore, it can be derived from (43) that

$$\begin{aligned}\Xi(T^-) =&e^{\mu_{\sigma(T^-)}T}V^{\sigma(T^-)}(Z(T))\\ \leq&\Xi(t_{\mathcal{N}^\sigma(0,T)})+\int_{t_{\mathcal{N}^\sigma(0,T)}}^{T} Ke^{\mu_{\sigma(t_{\mathcal{N}^\sigma(0,T)})}t}\mathrm{d}t\\ \leq&\Gamma_2\Xi(0)+\sum_{l=0}^{\mathcal{N}^\sigma(0,T)-1}\Gamma_{2,l}\int_{t_l}^{t_{l+1}} Ke^{\mu_{\sigma(t_l)}t}\mathrm{d}t+\int_{t_{\mathcal{N}^\sigma(0,T)}}^{T} Ke^{\mu_{\sigma(t_{\mathcal{N}^\sigma(0,T)})}t}\mathrm{d}t, \end{aligned} \tag{44}$$

where $\Gamma_2=\prod_{l=0}^{\mathcal{N}^\sigma(0,T)-1}\hbar_{\sigma(t_{l+1}),\sigma(t_l)}\exp\left\{\sum_{l=0}^{\mathcal{N}^\sigma(0,T)-1}(\mu_{\sigma(t_{l+1})}-\mu_{\sigma(t_l)})t_{l+1}\right\}$, $\Gamma_{2,l}=\prod_{s=l}^{\mathcal{N}^\sigma(0,T)-1}\hbar_{\sigma(t_{s+1}),\sigma(t_s)}\exp\left\{\sum_{s=l}^{\mathcal{N}^\sigma(0,T)-1}(\mu_{\sigma(t_{s+1})}-\mu_{\sigma(t_s)})t_{s+1}\right\}$.

Hence, from (44),

$$\begin{aligned}&V^{\sigma(T^-)}(Z(T))\\ \leq&\Gamma_3 V^{\sigma(0)}(Z(0))+\sum_{l=0}^{\mathcal{N}^\sigma(0,T)-1}\Gamma_{3,l}\int_{t_l}^{t_{l+1}} Ke^{\mu_{\sigma(t_l)}t}\mathrm{d}t+e^{-\mu_{\sigma(t_{\mathcal{N}^\sigma(0,T)})}T}\int_{t_{\mathcal{N}^\sigma(0,T)}}^{T} Ke^{\mu_{\sigma(t_{\mathcal{N}^\sigma(0,T)})}t}\mathrm{d}t\\ \leq&\overline{\Gamma}_3 V^{\sigma(0)}(Z(0))+\sum_{l=0}^{\mathcal{N}^\sigma(0,T)-1}\overline{\Gamma}_{3,l}e^{-\nu_{\min}t_{l+1}}\int_{t_l}^{t_{l+1}} Ke^{\nu_{\min}t}\mathrm{d}t+e^{-\nu_{\min}T}\int_{t_{\mathcal{N}^\sigma(0,T)}}^{T} Ke^{\nu_{\min}t}\mathrm{d}t\\ \leq&\widetilde{\Gamma}_3 V^{\sigma(0)}(Z(0))+\sum_{l=0}^{\mathcal{N}^\sigma(0,T)-1}\widetilde{\Gamma}_{3,l}e^{-\nu_{\min}t_{l+1}}\int_{t_l}^{t_{l+1}} Ke^{\nu_{\min}t}\mathrm{d}t+e^{-\nu_{\min}T}\int_{t_{\mathcal{N}^\sigma(0,T)}}^{T} Ke^{\nu_{\min}t}\mathrm{d}t, \end{aligned} \tag{45}$$

where $\Gamma_3=\prod_{l=0}^{\mathcal{N}^\sigma(0,T)-1}\hbar_{\sigma(t_{l+1}),\sigma(t_l)}\exp\left\{-\mu_{\sigma(t_{\mathcal{N}^\sigma(0,T)})}T+\sum_{l=0}^{\mathcal{N}^\sigma(0,T)-1}(\mu_{\sigma(t_{l+1})}-\mu_{\sigma(t_l)})t_{l+1}+\mu_{\sigma(t_0)}t_0\right\}$, $\Gamma_{3,l}=\prod_{s=l}^{\mathcal{N}^\sigma(0,T)-1}\hbar_{\sigma(t_{s+1}),\sigma(t_s)}\exp\left\{-\mu_{\sigma(t_{\mathcal{N}^\sigma(0,T)})}T+\sum_{s=l}^{\mathcal{N}^\sigma(0,T)-1}(\mu_{\sigma(t_{s+1})}-\mu_{\sigma(t_s)})t_{s+1}\right\}$, $\overline{\Gamma}_3=\prod_{p=1}^{M}\prod_{q=1,q\neq p}^{M}\hbar_{p,q}^{\mathcal{N}_{p,q}^\sigma(0,T)}\exp\left\{-\sum_{p=1}^{M}\sum_{q=1,q\neq p}^{M}\mu_p\sum_{s\in\beta_{(p,q)}}(t_{s+1}-t_s)-\mu_{\sigma(t_{\mathcal{N}^\sigma(0,T)})}(T-\right.$

$t_{\mathcal{N}^\sigma(0,T)})\Big\}$, $\overline{\Gamma}_{3,l} = \prod_{s=l}^{\mathcal{N}^\sigma(0,T)-1} \hbar_{\sigma(t_{s+1}),\sigma(t_s)} \exp\Big\{\mu_{\sigma(t_l)}t_{l+1} + \sum_{s=l}^{\mathcal{N}^\sigma(0,T)-1}(\mu_{\sigma(t_{s+1})} - \mu_{\sigma(t_s)})t_{s+1} - \mu_{\sigma(t_{\mathcal{N}^\sigma(0,T)})}T\Big\}$, $\widetilde{\Gamma}_3 = \exp\Big\{\sum_{p=1}^M \sum_{q=1,q\neq p}^M \Big[\Big(\mathcal{N}_{p,q}^0 + \frac{T_{p,q}(0,T)}{\tau_{p,q}^a}\Big)\ln\hbar_{p,q} - \mu_p T_{p,q}(0,T)\Big]\Big\}$, $\widetilde{\Gamma}_{3,l} = \prod_{p=1}^M \prod_{q=1,q\neq p}^M \hbar_{p,q}^{\mathcal{N}_{p,q}^\sigma(t_{l+1},T)} \exp\Big\{-\sum_{p=1}^M \sum_{q=1,q\neq p}^M \mu_p T_{p,q}(t_{l+1},T)\Big\}$, $\beta_{(p,q)}$ stands for the set of satisfying $\sigma(t_s) = p$, $\sigma(t_s^-) = q$, $t_s \in \{t_0, t_1, \ldots, t_k, t_{k+1}, \ldots, t_{\mathcal{N}^\sigma(0,T)-1}\}$, and $\nu_{p,q} \in (0, \mu_p - \ln\hbar_{p,q}/\tau_{p,q}^a)$ with $\nu_{\min} = \min_{p,q\in\Omega}\{\nu_{p,q}\}$.

Utilizing $\tau_{p,q}^a > \frac{\ln\hbar_{p,q}}{\mu_p}$, for any $T \geq t \geq 0$,

$$\mathcal{N}_{p,q}^\sigma(t,T) \leq \mathcal{N}_{p,q}^0 + \frac{(\mu_p - \nu_{p,q})T_{p,q}(t,T)}{\ln\hbar_{p,q}},$$

which implies

$$\hbar_{p,q}^{\mathcal{N}_{p,q}^\sigma(t_{l+1},T)} \leq \hbar_{p,q}^{\mathcal{N}_{p,q}^0} e^{(\mu_p-\nu_{p,q})T_{p,q}(t_{l+1},T)}. \tag{46}$$

According to (45) and (46), it's easy to verify that

$$\begin{aligned} V^{\sigma(T^-)}(Z(T)) \leq & \Gamma_4 V^{\sigma(0)}(Z(0)) + \prod_{p=1}^M \prod_{q=1,q\neq p}^M \hbar_{p,q}^{\mathcal{N}_{p,q}^0} e^{-\nu_{\min}T} \int_0^T K e^{\nu_{\min}t}\mathrm{d}t \\ \leq & e^{\sum_{p=1}^M \sum_{q=1,q\neq p}^M \mathcal{N}_{p,q}^0 \ln\hbar_{p,q}} \max_{p,q\in\Omega}\Big\{\frac{\ln\hbar_{p,q}}{\tau_{p,q}^a} - \mu_p\Big\}^T V^{\sigma(0)}(Z(0)) + \frac{K}{\nu_{\min}} \prod_{p=1}^M \prod_{q=1,q\neq p}^M \hbar_{p,q}^{\mathcal{N}_{p,q}^0}, \end{aligned} \tag{47}$$

where $\Gamma_4 = \exp\Big\{\sum_{p=1}^M \sum_{q=1,q\neq p}^M \Big(\mathcal{N}_{p,q}^0 \ln\hbar_{p,q} + \Big(\frac{\ln\hbar_{p,q}}{\tau_{p,q}^a} - \mu_p\Big) T_{p,q}(0,T)\Big)\Big\}$.

Therefore, we can deduce from (47) that all signals in the closed-loop system are bounded. Since $\xi_i \in \mathcal{L}_\infty$ is ensured, the system state x_{ik} always remains in the predefined constraint set $\mathcal{D}_{ik}$, $i = 1, 2$, and $k = 1, \ldots, m$, under the initial condition $x_{ik}(0) \in \mathcal{D}_{ik}$. This implies that there exist positive constants $\overline{D}_{i,k}^*$, $\underline{D}_{i,k}^*$ such that $-\underline{D}_{i,k} < -\underline{D}_{i,k}^* \leq x_{ik} \leq \overline{D}_{i,k}^* < \overline{D}_{i,k}$, $i = 1, 2$, and $k = 1, \ldots, m$, namely, the FSCs (2) are always maintained without imposing the feasibility condition on the virtual control law α_1. Moreover, according to the definition of $z_{1k} = \xi_{1k} - \alpha_{1f,k} = \frac{\overline{D}_{1k}\underline{D}_{1k}x_{1k}}{(\overline{D}_{1k}-x_{1k})(\underline{D}_{1k}+x_{1k})} - \frac{\overline{D}_{1k}\underline{D}_{1k}y_{dk}}{(\overline{D}_{1k}-y_{dk})(\underline{D}_{1k}+y_{dk})}$, $k = 1, \ldots, m$, the tracking error variable $x_{1k} - y_{dk} = e_k = \eta_k z_{1k}$, where $\eta_k = \frac{(\overline{D}_{1k}-x_{1k})(\underline{D}_{1k}+x_{1k})(\overline{D}_{1k}-y_{dk})(\underline{D}_{1k}+y_{dk})}{\overline{D}_{1k}\underline{D}_{1k}(\overline{D}_{1k}\underline{D}_{1k}+x_{1k}y_{dk})}$. Since $y_{dk} \in \mathcal{D}_{dk} \subsetneqq \mathcal{D}_{1k}$ and $-\underline{D}_{1,k} < -\underline{D}_{1,k}^* \leq x_{1k} \leq \overline{D}_{1,k}^* < \overline{D}_{1,k}$, $k = 1, \ldots, m$, there exist positive constants $\overline{\eta}_k$, $\underline{\eta}_k$ such that $\underline{\eta}_k \leq \eta_k \leq \overline{\eta}_k$, which means that e_k are bounded for $t \geq 0$. In fact, from (39), we have $\dot{V}^p \leq -c_1\|z_1\|^2 + K$, which indicates that $\dot{V}^p$ becomes negative when $\|z_1\| > \left(\frac{K+\delta}{c_1}\right)^{\frac{1}{2}}$ with δ being a small constant. Consequently, $\|z_1\|$ will enter and stay within the compact set $\Omega_{z_1} = \left\{z_1 \in \mathbb{R}^m \,\middle|\, \|z_1\| \leq \left(\frac{K+\delta}{c_1}\right)^{\frac{1}{2}}\right\}$, which implies that the tracking error e will enter and remain within the compact set $\Omega_e = \left\{e \in \mathbb{R}^m \,\middle|\, \|e\| \leq \overline{\eta}\left(\frac{K+\delta}{c_1}\right)^{\frac{1}{2}}\right\}$, where $\overline{\eta} = \max\{\overline{\eta}_k\}$ for $k = 1, \cdots, m$. This completes the proof. ∎

Remark 6 *When $\underline{D}_{ik} = \overline{D}_{ik}$ holds for $i = 1, 2$, and $k = 1, \ldots, m$, the case of asymmetric SCs (2) reduces to the case of symmetric SCs. Moreover, when $\underline{D}_{ik}$ and $\overline{D}_{ik}$ divergence to infinity (indicating no SCs in control requirements), our analysis in Remark 2 demonstrates that the parameters reduce to $\xi_{ik} = x_{ik}$, $\lambda_{ik} = 1$, $\rho_{ik} = 1$, and $\alpha_{1f,k} = y_{dk}$. In order to achieve the control goal in the unconstrained scenario, the algorithm designed in this paper only needs to be simplified to substitute ξ_{ik}, λ_{ik}, ρ_{ik}, and $\alpha_{1f,k}$ into their corresponding values x_{ik}, 1, 1, and y_{dk} respectively, so as to keep the original controller architecture and all design parameters unchanged.*

3.3 The Case of Time-Varying Constraints

Time-varying constraints are important in practical applications where safety limits, operational envelopes, or performance requirements evolve over time, such as actuator aging, environmental changes, or task-dependent safety margins. To reflect these realistic scenarios, the constraint bounds $\overline{D}_{ik}$ and $\underline{D}_{ik}$ are introduced as bounded $\mathcal{C}^2$ functions (see Assumption 4).

Assumption 4 [32] *The positive time-varying constraint functions $\overline{D}_{ik}(t)$ and $\underline{D}_{ik}(t)$, $i = 1, 2$, and $k = 1, \ldots, m$, are bounded and of class $\mathcal{C}^2$ with the first and second derivatives bounded.*

Assumption 5 [32] *The desired signal vectors y_d, $\dot{y}_d$, $\ddot{y}_d$ are available and continuous in known compact set $\mathcal{D}_d := \{[y_d^{\mathrm{T}}, \dot{y}_d^{\mathrm{T}}, \ddot{y}_d^{\mathrm{T}}]^{\mathrm{T}} | y_d^{\mathrm{T}} y_d + \dot{y}_d^{\mathrm{T}} \dot{y}_d + \ddot{y}_d^{\mathrm{T}} \ddot{y}_d \leq D_0\}$ with D_0 being a positive constant. Moreover, there exist positive constants $\overline{D}_{dk}$, $\underline{D}_{dk}$, $k = 1, \ldots, m$, satisfying $y_{dk} \in \mathcal{D}_{dk} := \{-\underline{D}_{1k}(t) < -\underline{D}_{dk} \leq y_{dk} \leq \overline{D}_{dk} < \overline{D}_{1k}(t)\}$.*

To deal with the more general case of time-varying asymmetric FSCs, introduce a NTF as follows:

$$\xi_{ik} = \frac{\overline{D}_{ik}(t)\underline{D}_{ik}(t)x_{ik}}{(\overline{D}_{ik}(t) - x_{ik})(\underline{D}_{ik}(t) + x_{ik})}, \tag{48}$$

where $\overline{D}_{ik}(t)$ and $\underline{D}_{ik}(t)$ are time-varying positive functions satisfying $-\underline{D}_{ik}(0) < x_{ik}(0) < \overline{D}_{ik}(0)$, $i = 1, 2$, and $k = 1, \ldots, m$. In the following, $\overline{D}_{ik}(t)$ and $\underline{D}_{ik}(t)$ are simply denoted as $\overline{D}_{ik}$ and $\underline{D}_{ik}$, respectively. Then, the derivative of ξ_{ik} can be expressed as :

$$\dot{\xi}_{ik} = \bar{\lambda}_{i1,k}\dot{x}_{ik} + \bar{\lambda}_{i2,k}, \tag{49}$$

where $\bar{\lambda}_{i1,k} = \frac{\overline{D}_{ik}\underline{D}_{ik}(\overline{D}_{ik}\underline{D}_{ik}+x_{ik}^2)}{(\overline{D}_{ik}-x_{ik})^2(\underline{D}_{ik}+x_{ik})^2}$ and $\bar{\lambda}_{i2,k} = \frac{(\overline{D}_{ik}^2\dot{\underline{D}}_{ik} - \dot{\overline{D}}_{ik}\underline{D}_{ik}^2 - (\overline{D}_{ik}\dot{\underline{D}}_{ik} + \dot{\overline{D}}_{ik}\underline{D}_{ik})x_{ik})x_{ik}^2}{(\overline{D}_{ik}-x_{ik})^2(\underline{D}_{ik}+x_{ik})^2}$ are well defined and calculable for $-\underline{D}_{ik} < x_{ik} < \overline{D}_{ik}$, $t \geq 0$, $i = 1, 2$, and $k = 1, \ldots, m$.

Based on the time-varying NTF (48) and the change of coordinates (7), we propose the corresponding control strategy

$$\begin{cases} \alpha_1 = -(c_1 + \widehat{\Theta}\Psi_1^*)(\lambda_1^*)^{-2}\bar{\lambda}_{11}z_1 \\ u = -\left(c_2 + \frac{\widehat{\Theta}}{g_{2,m}^p}\Psi_2^*\right)(\lambda_2^*)^{-2}\bar{\lambda}_P^{-1}\bar{\lambda}_{21}Pz_2 \\ \Psi_1^* = \frac{1}{2a^2}\left(\|\bar{\lambda}_{11}\|^2\varphi_1 + \|\bar{\lambda}_{12} - \bar{\lambda}_{d1}\dot{y}_d - \bar{\lambda}_{d2}\|^2 + \frac{(g_{1,\max})^2}{(g_{1,\min})^2}\|\bar{\lambda}_{11}\|^2\right) \\ \Psi_2^* = \frac{1}{2a^2}\left(\|P\|^2\|\bar{\lambda}_{21}\|^2\varphi_2 + \|P\|^2\|E(\varepsilon)(\bar{\lambda}_{22} - \dot{\alpha}_{2f})\|^2 + \|z_1\|^2\|\bar{\lambda}_{11}\|^2\|\rho_2\|^2\right) \end{cases} \tag{50}$$

with the adaptive law

$$\dot{\widehat{\Theta}} = \gamma \left(\Psi_1^* \|z_1\|^2 + \frac{1}{g_{2,\min}} \Psi_2^* \|z_2\|^2 \right) - l\widehat{\Theta}, \tag{51}$$

where c_1, c_2, γ, l, a are the positive design parameters and P is defined in (26). For $i = 1, 2, p \in \Omega$, z_i is defined in (7), $\|\varphi_i^p\|^2 \leq \varphi_i$, $\widetilde{\Theta} = \Theta - \widehat{\Theta}$ is the parameter estimate error with $\widehat{\Theta}$ being the parameter estimate of Θ and $\Theta = \max\{(b_i^p)^2, 1\}$. For $i = 1, 2$, and $k = 1, \ldots, m$, $\bar{\lambda}_{i1} = \mathrm{diag}\{\bar{\lambda}_{i1,1}, \ldots, \bar{\lambda}_{i1,m}\}$, $\bar{\lambda}_{i2} = [\bar{\lambda}_{i2,1}, \ldots, \bar{\lambda}_{i2,m}]^{\mathrm{T}}$, $\bar{\lambda}_{d1} = \mathrm{diag}\{\bar{\lambda}_{d1,1}, \ldots, \bar{\lambda}_{d1,m}\}$ with $\bar{\lambda}_{d1,k} = \frac{\overline{D}_{1k}\underline{D}_{1k}(\overline{D}_{1k}\underline{D}_{1k} + y_{dk}^2)}{(\overline{D}_{1k} - y_{dk})^2(\underline{D}_{1k} + y_{dk})^2}$, $\bar{\lambda}_{d2} = [\bar{\lambda}_{d2,1}, \ldots, \bar{\lambda}_{d2,m}]^{\mathrm{T}}$ with $\bar{\lambda}_{d2,k} = \frac{(\overline{D}_{1k}^2 \dot{\underline{D}}_{1k} - \dot{\overline{D}}_{1k}\underline{D}_{1k}^2 - (\overline{D}_{1k}\dot{\underline{D}}_{1k} + \dot{\overline{D}}_{1k}\underline{D}_{1k}) y_{dk}) y_{dk}^2}{(\overline{D}_{1k} - y_{dk})^2(\underline{D}_k + y_{dk})^2}$, $\lambda_1^* = \min\{\lambda_{1k}^*\}$ with $\lambda_{1k}^* = \frac{16\overline{D}_{1k}^2\underline{D}_{1k}^2}{(\overline{D}_{1k} + \underline{D}_{1k})^4}$, $\lambda_2^* = \min\{\lambda_{2k}^*\}$ with $\lambda_{2k}^* = \frac{16\overline{D}_{2k}^2\underline{D}_{2k}^2}{(\overline{D}_{2k} + \underline{D}_{2k})^4}$, $\bar{\lambda}_P = \lambda_{\min}(P^2)$, $\rho_2 = \mathrm{diag}\{\rho_{21}, \ldots, \rho_{2m}\}$ with $\rho_{2k} = \frac{(\overline{D}_{2k} - x_{2k})(\underline{D}_{2k} + x_{2k})}{\overline{D}_{2k}\underline{D}_{2k}}$, $g_{1,\min} = \min_{p\in\Omega}\{g_{1,m}^p\}$, $g_{1,\max} = \max_{p\in\Omega}\{g_{1,M}^p\}$, $g_{2,\min} = \min_{p\in\Omega}\{g_{2,m}^p\}$.

Next, we declare the following conclusion on the time-varying asymmetric FSCs.

Theorem 2 *Consider the uncertain switched TTSSs (1) with time-varying asymmetric FSCs* $-\underline{D}_{ik}(t) < x_{ik} < \overline{D}_{ik}(t)$, $i = 1, 2$, *and* $k = 1, \ldots, m$, *under the control strategy (50) and (51). Let the Lyapunov function candidate be designed as (31). If* $-\underline{D}_{ik}(0) < x_{ik}(0) < \overline{D}_{ik}(0)$, $i = 1, 2$, *and* $k = 1, \ldots, m$, *the AED-ADT of the switching signal* $\sigma(t)$ *satisfies* $\tau_{p,q}^a > \frac{\ln \hbar_{p,q}}{\mu_p}$, *and there exists a positive constant* B_0 *such that* $V^p(0) \leq B_0$, $p \in \Omega$, *then under Assumptions 2-5, the control objectives* P_1*-*P_3 *can be achieved through the single-parameter-estimation-based adaptive control.*

Proof: The proof can be conducted similarly to the proof of Theorem 1. ∎

4 Simulation Results

In this section, the efficacy of the proposed control method is demonstrated through numerical simulations.

Example 1: Consider the following uncertain switched TTSSs (1), where $m = 2$, $\sigma(t) : [0, +\infty) \to \Omega = \{1, 2, 3\}$, and F_i^p, G_i^p, $i = 1, 2, p = 1, 2, 3$, are given as:

$$F_1^1 = \begin{bmatrix} \theta_{11} x_{11} \sin(x_{11}) \\ 0.1 x_{11} x_{12} \cos(\theta_{12} t) \end{bmatrix}, \quad F_1^2 = \begin{bmatrix} \theta_{11} x_{11} \\ x_{12} e^{-\theta_{12} t} \end{bmatrix}, \quad F_1^3 = \begin{bmatrix} \theta_{11} \cos(x_{11}) \\ \theta_{12} x_{12} \end{bmatrix},$$

$$F_2^1 = \begin{bmatrix} x_{21} e^{-\theta_{21} t} \\ \theta_{22} x_{11} x_{22}^2 \end{bmatrix}, \quad F_2^2 = \begin{bmatrix} 0.1 x_{11} x_{21} \sin(\theta_{21} t) \\ \theta_{22} x_{22} \end{bmatrix}, \quad F_2^3 = \begin{bmatrix} 0.1 x_{21} \sin(\theta_{21} t) \\ \theta_{22} x_{22}^2 \end{bmatrix}$$

and

$$G_1^1 = \begin{bmatrix} 1.2 + 0.4 e^{-x_{11}} & 0.5 \\ 0.5 & 1 + 0.5 \cos^2(x_{12}) \end{bmatrix}, \quad G_2^1 = \begin{bmatrix} 2 + 0.2 \sin(x_{11}^2) & 0.6 \\ 0.6 & 1.5 + 0.5 e^{-x_{22}} \end{bmatrix},$$

$$G_1^2 = \begin{bmatrix} 1 + 0.1 \sin(x_{11}^2) & 0.4 \sin(x_{12}) \\ 0.4 \sin(x_{12}) & 1.8 + 0.2 e^{-x_{12}} \end{bmatrix}, \quad G_2^2 = \begin{bmatrix} 1.2 & 0.4 \sin(x_{21}) \\ 0.4 \sin(x_{21}) & 1.4 \end{bmatrix},$$

$$G_1^3 = \begin{bmatrix} 0.8 + 0.6 e^{-x_{11}} & 0.4 \tanh(x_{11} x_{12}) \\ 0.4 \tanh(x_{11} x_{12}) & 1.4 + 0.2 \sin(x_{12}^2) \end{bmatrix}, \quad G_2^3 = \begin{bmatrix} 5 + 0.1 e^{-x_{21}} & 0.5 \arctan(x_{11}) \\ 0.5 \arctan(x_{11}) & 2 + \sin^2(x_{22}) \end{bmatrix},$$

where $\theta_1 = [\theta_{11}, \theta_{12}]^{\mathrm{T}} = [0.15, 0.2]^{\mathrm{T}}$, $\theta_2 = [\theta_{21}, \theta_{22}]^{\mathrm{T}} = [0.2, 0.1]^{\mathrm{T}}$, and $\varepsilon = 0.05$.

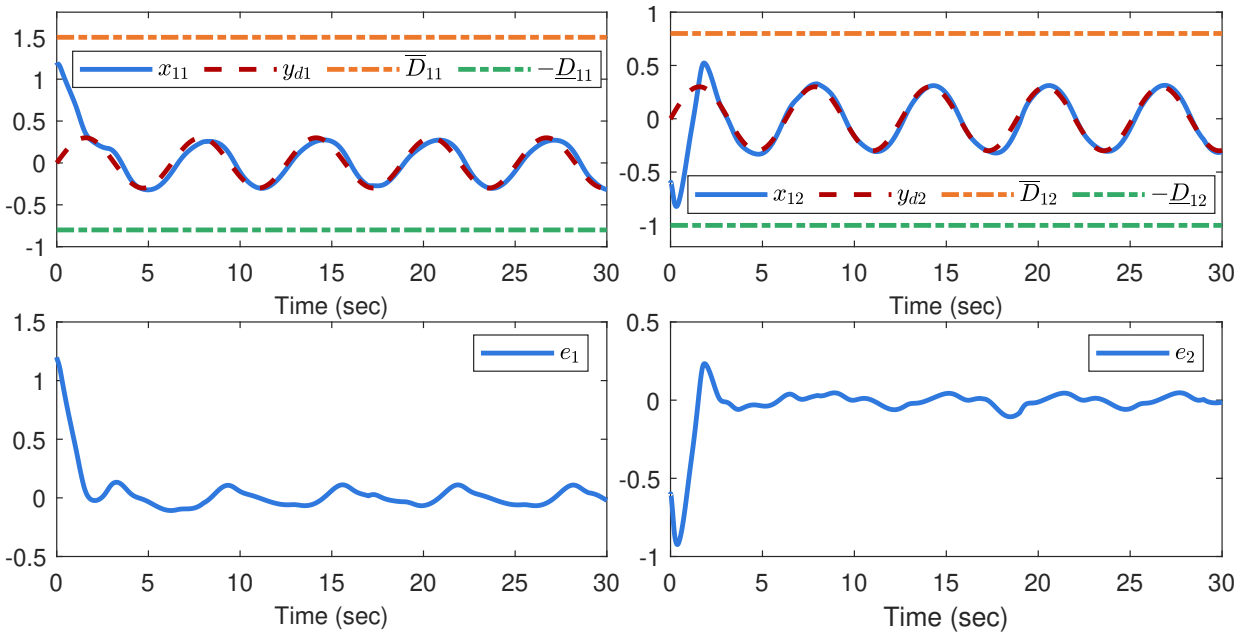


Figure 1: Trajectories of the system state $x_1 = [x_{11}, x_{12}]^{\mathrm{T}}$ and the desired signal $y_d = [y_{d1}, y_{d2}]^{\mathrm{T}}$ under SCs (52), and the tracking error $e = [e_1, e_2]^{\mathrm{T}}$ in Example 1.

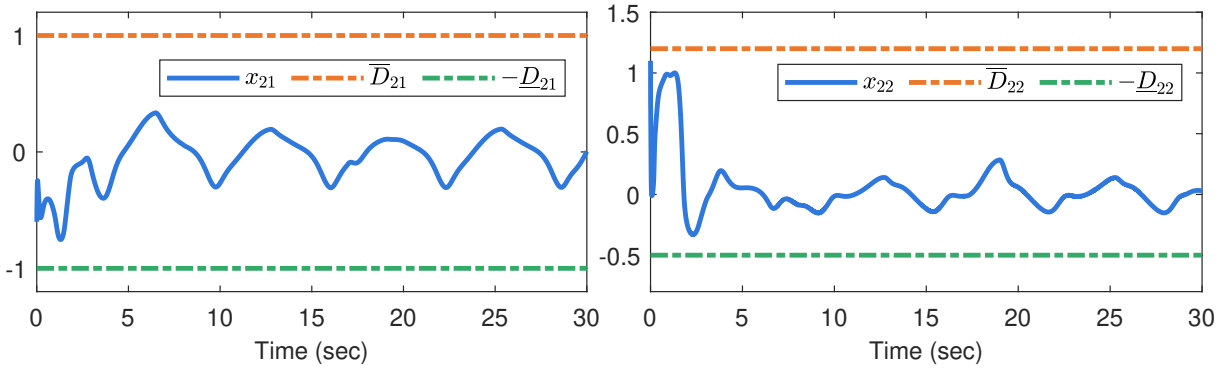


Figure 2: Trajectory of the system state $x_2 = [x_{21}, x_{22}]^{\mathrm{T}}$ under SCs (52) in Example 1.

The control objectives are: (i) all signals in the closed-loop system are bounded and the output y tracks the desired trajectory $y_d = [y_{d1}, y_{d2}]^{\mathrm{T}} = [0.3\sin(t), 0.3\sin(t)]^{\mathrm{T}}$ to a bounded compact set, and (ii) the system states are constrained in the following sets:

$$x_{ik} \in \mathcal{D}_{ik} := \{x_{ik} \in \mathbb{R} | -\underline{D}_{ik} < x_{ik} < \overline{D}_{ik}\}, \tag{52}$$

for $i = 1, 2, k = 1, 2$, where $\overline{D}_{11} = 1.5$, $\underline{D}_{11} = 0.8$, $\overline{D}_{12} = 0.8$, $\underline{D}_{12} = 1$, $\overline{D}_{21} = 1$, $\underline{D}_{21} = 1$, $\overline{D}_{22} = 1.2$, $\underline{D}_{22} = 0.5$. To ensure that the FSCs (52) are not violated, the initial states are given as $x_1(0) = [x_{11}(0), x_{12}(0)]^{\mathrm{T}} = [1.2, -0.6]^{\mathrm{T}}$, $x_2(0) = [x_{21}(0), x_{22}(0)]^{\mathrm{T}} = [-0.6, 1.1]^{\mathrm{T}}$ and the initial estimate value is $\widehat{\Theta}(0) = 0$. The design parameters are selected according to the sufficient conditions

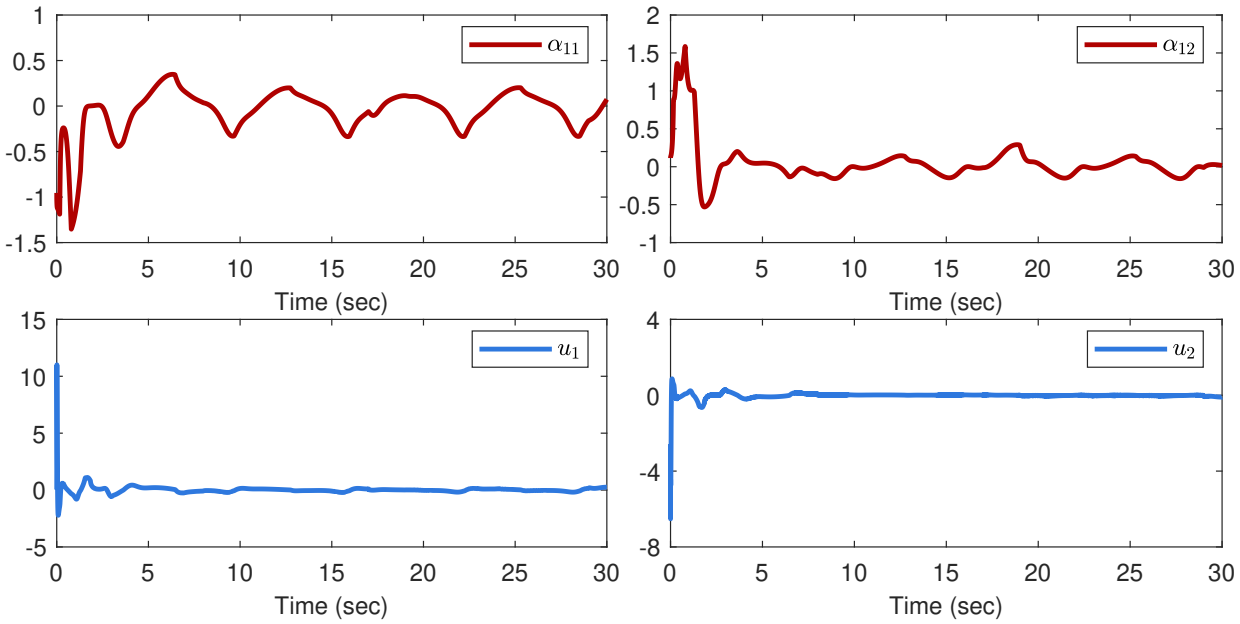


Figure 3: Trajectories of the virtual control $\alpha_1 = [\alpha_{11}, \alpha_{12}]^{\mathrm{T}}$ and the control input $u = [u_1, u_2]^{\mathrm{T}}$ in Example 1.

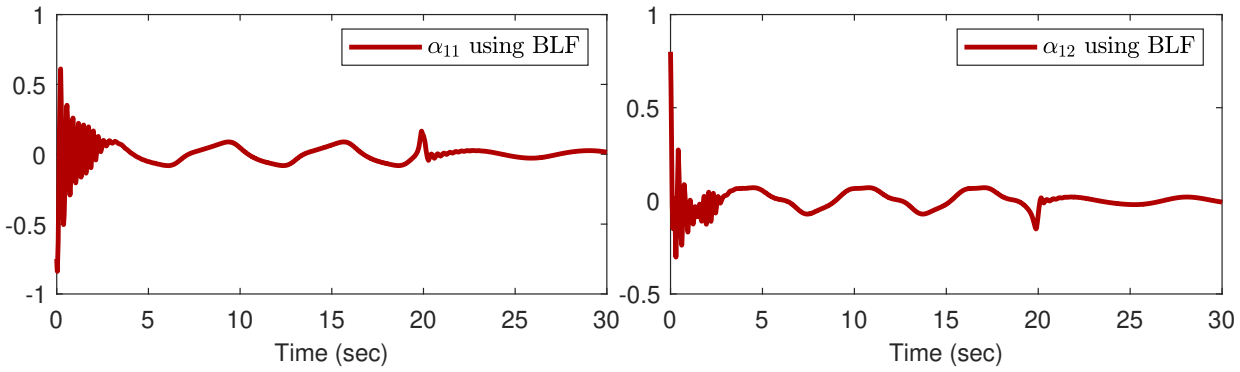


Figure 4: Trajectories of the virtual control $\alpha_1 = [\alpha_{11}, \alpha_{12}]^{\mathrm{T}}$ using BLF methods in [24–26].

obtained in the stability analysis. A practical selection procedure is summarized as follows:

Step 1: the positive definite matrix P is selected, and the feedback gains c_1 and c_2 are chosen as positive constants. Larger values of c_1 and c_2 generally increase the decay rates of z_1 and z_2, respectively, as can be seen from (35).

Step 2: the filter parameter κ_2 is selected to satisfy the condition given below (23), while a is used to balance the terms introduced by Young's inequality. The parameters γ and l determine the adaptation behavior and are further adjusted according to the desired transient performance. After these parameters are fixed, μ_p and $\hbar_{p,q}$ are calculated from (36) and (37), respectively.

Step 3: the admissible AED-ADT bounds are obtained according to the condition $\tau^a_{p,q} > \ln \hbar_{p,q}/\mu_p$ in Theorem 1. Following this procedure, the parameters used in this example are selected as $c_1 = 3.5$, $c_2 = 3$, $\gamma = 0.1$, $l = 0.2$, $\kappa_2 = 0.2$, $a = 3$, and $P_{11} = P_{22} = 1$. Accordingly, from (36), (37),

Table 1: Example 1 under AED-ADT switching, MDADT switching, and ADT switching.

Switching strategies	**AED-ADT**	**MDADT in [8]**	**ADT in [39]**
	$\hbar_{1,2} = 1.3751$		
	$\hbar_{1,3} = 2.5001$		
	$\hbar_{2,1} = 1.6665$		
	$\hbar_{2,3} = 4.1665$	$\hbar_1 = 2.5001$	
	$\hbar_{3,1} = 1.3332$	$\hbar_2 = 4.1665$	
	$\hbar_{3,2} = 1.8333$	$\hbar_3 = 1.8333$	
Switching	$\mu_1 = 0.2$	$\mu_1 = 0.2$	$\hbar = 4.1665$
signals	$\mu_2 = 0.2$	$\mu_2 = 0.2$	$\mu = 0.2$
	$\mu_3 = 0.2$	$\mu_3 = 0.2$	$\tau^a \geq 7.1354$
	$\tau^a_{1,2} \geq 1.5926$	$\tau^a_1 \geq 4.5817$	
	$\tau^a_{1,3} \geq 4.5817$	$\tau^a_2 \geq 7.1354$	
	$\tau^a_{2,1} \geq 2.5536$	$\tau^a_3 \geq 3.0306$	
	$\tau^a_{2,3} \geq 7.1354$		
	$\tau^a_{3,1} \geq 1.4379$		
	$\tau^a_{3,2} \geq 3.0306$		

and Theorem 1, we obtain $\tau^a_{1,2} \geq 1.5926$, $\tau^a_{1,3} \geq 4.5817$, $\tau^a_{2,1} \geq 2.5536$, $\tau^a_{2,3} \geq 7.1354$, $\tau^a_{3,1} \geq 1.4379$, and $\tau^a_{3,2} \geq 3.0306$.

The simulation results are depicted in Figs. 1-4. Fig. 1 illustrates the trajectories of the system state $x_1 = [x_{11}, x_{12}]^{\mathrm{T}}$ and the desired signal $y_d = [y_{d1}, y_{d2}]^{\mathrm{T}}$ under SCs (52), and the tracking error $e = [e_1, e_2]^{\mathrm{T}}$. The trajectory of the system state $x_2 = [x_{21}, x_{22}]^{\mathrm{T}}$ under SCs (52) is exhibited in Fig. 2. This indicates that the system states remain in the predefined regions under the proposed control method, and the tracking error converges to a bounded compact set. Moreover, the trajectories of the virtual control $\alpha_1 = [\alpha_{11}, \alpha_{12}]^{\mathrm{T}}$ and the control input u are shown in Fig. 3. Note that if the BLF methods in [24–26] are applied to Example 1, the feasibility conditions on the virtual controls α_{11}, α_{12} need to be satisfied, i.e., $-1 < \alpha_{11} < 1, -0.5 < \alpha_{12} < 1.2$ (see Fig. 4). However, as shown in Fig. 3, our control scheme can work effectively even if the virtual controls α_{11}, α_{12} do not fall within the predefined constraints, which enhances the accessibility and ease in the design of the proposed control scheme.

Remark 7 *In order to facilitate comparison, we give the results of Example 1 in Table 1, based on the AED-ADT switching, the MDADT switching in [8], and the ADT switching in [39] with the same initial conditions and control targets. It can be inferred that the calculated ADT* $\tau^a \geq 7.1354$ *and the calculated MDADT* $\tau^a_1 \geq 4.5817$, $\tau^a_2 \geq 7.1354$, $\tau^a_3 \geq 3.0306$, *are significantly greater than or equal to the calculated AED-ADT* $\tau^a_{1,2} \geq 1.5926$, $\tau^a_{1,3} \geq 4.5817$, $\tau^a_{2,1} \geq 2.5536$, $\tau^a_{2,3} \geq 7.1354$,

$\tau_{3,1}^a \geq 1.4379$, $\tau_{3,2}^a \geq 3.0306$, *which shows that AED-ADT switching offers greater flexibility and effectively encompasses both ADT and MDADT switching as special cases.*

Example 2: Consider a DC motor system in [14] where the electromagnetic transient characteristics are much faster than the torque response. The dynamics of the system is described by

$$\begin{cases} \mathcal{J}_m \frac{\mathrm{d}\omega}{\mathrm{d}t} = -b_{\sigma(t)}\omega + k_m i \\ \mathcal{L}\frac{\mathrm{d}i}{\mathrm{d}t} = -k_b\omega - \mathcal{R}_0 i + u \\ y = \omega \end{cases} \tag{53}$$

where ω is the angle speed, i, $\mathcal{R}_0$, and u are the armature current, resistance, and voltage, respectively, $\mathcal{J}_m$ denotes the equivalent moment of inertia, $\mathcal{L}$ is a small constant representing the inductance, k_m and k_b are the torque and back electromotive force, $b_{\sigma(t)}$ is the equivalent viscous friction coefficient and $\sigma(t) : [0, +\infty) \to \Omega = \{1, 2, 3\}$. Let $\mathcal{R}_0 = 0.6\Omega$, $\mathcal{J}_m = 0.093\mathrm{kg} \cdot \mathrm{m}^2$, $\mathcal{L} = 0.06\mathrm{H}$, $k_m = 0.7274\mathrm{N} \cdot \mathrm{m}$, $k_b = 0.6\mathrm{v} \cdot \mathrm{s/rad}$, $b_1 = 0.006$, $b_2 = 0.008$, $b_3 = 0.01$.

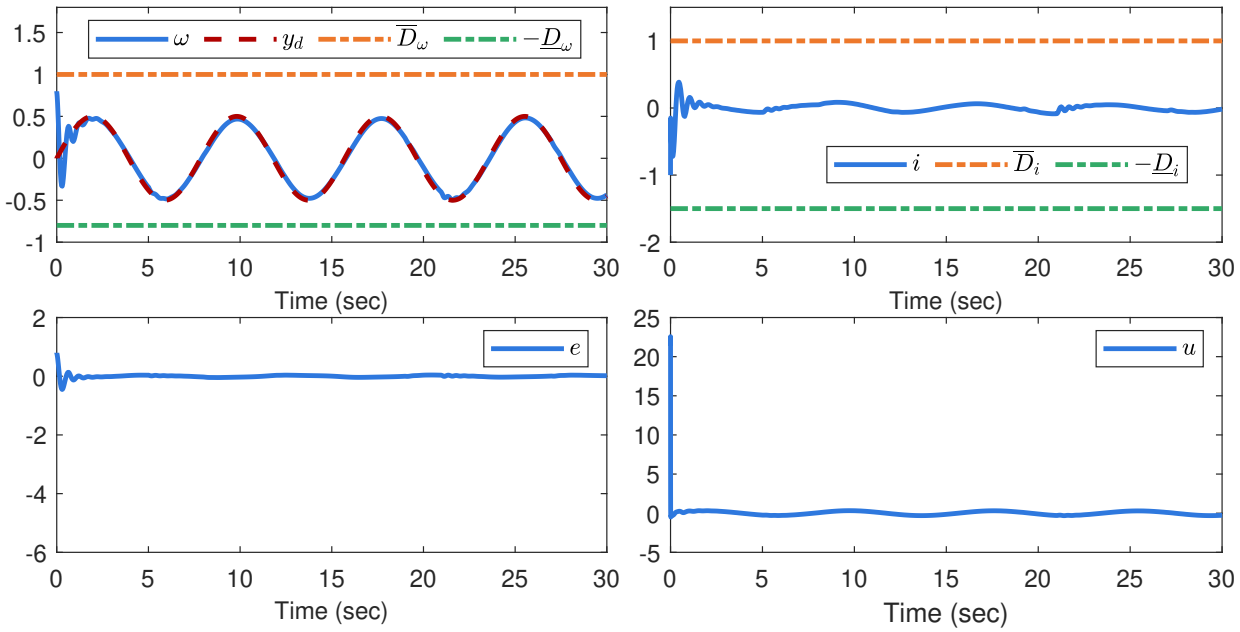


Figure 5: Trajectories of the angle speed ω, the armature current i and the desired signal y_d under SCs (54), the tracking error e, and the control input u in Example 2.

The control objectives are: (i) all signals in the closed-loop system are bounded and the output y tracks the desired trajectory $y_d = 0.5\sin(0.8t)$ as closely as possible, and (ii) the system states are constrained in the following sets:

$$\begin{aligned} \omega \in \mathcal{D}_\omega &:= \{\omega \in \mathbb{R} | -\underline{D}_\omega < \omega < \overline{D}_\omega\}, \\ i \in \mathcal{D}_i &:= \{i \in \mathbb{R} | -\underline{D}_i < i < \overline{D}_i\}, \end{aligned} \tag{54}$$

where $\overline{D}_\omega = 1$, $\underline{D}_\omega = 0.8$, $\overline{D}_i = 1$, $\underline{D}_i = 1.5$. In order to guarantee that the SCs (54) are not violated, the initial states are taken as $\omega(0) = 0.8$, $i(0) = -1$. Following the same parameter selection procedure described in Example 1, the design parameters are selected as $c_1 = 5$, $c_2 = 2$, $\kappa_2 = 0.2$, $a = 1$, and $P = 1$. Then, according to (36), (37), and Theorem 1, the corresponding AED-ADT bounds are obtained as $\tau^a_{1,2} \geq 2.7184$, $\tau^a_{1,3} \geq 3.2959$, $\tau^a_{2,1} \geq 6.0412$, $\tau^a_{2,3} \geq 1.9845$, $\tau^a_{3,1} \geq 5.6723$, and $\tau^a_{3,2} \geq 3.3301$. The trajectories of the angle speed ω, the armature current i and the desired signal y_d under SCs (54), the tracking error e, and the control input u are depicted in Fig. 5, demonstrating the efficacy of the proposed control method.

5 Conclusion

In this paper, the adaptive tracking problem is investigated for uncertain switched TTSSs under the AED-ADT switching law with SCs. First, the SCs are solved by constructing the NTF and the change of coordinates on the system states to eliminate the requirement of the feasibility conditions on the virtual controls. Then, utilizing a mode-dependent and ε-dependent Lyapunov function, a single-parameter-estimation-based state feedback controller is proposed while the adaptive law is mode-independent under a class of switching signals with the AED-ADT property. Finally, the theoretical results are validated through two numerical examples. Several directions are worth further investigation. First, the output feedback control problem for switched TTSSs with SCs will be studied when some system states are not directly measurable. Second, less conservative switching conditions and more general switching mechanisms will be explored to further improve the flexibility of the proposed method. In addition, experimental studies on practical systems will be considered to further verify the effectiveness and applicability of the proposed control scheme.

Acknowledgments

This work was supported by the National Natural Science Foundation of China under Grants 62473164, 62173152, and the Fundamental Research Funds for the Central Universities under grant 2024BRA014.

Conflict of interest

We declare that we have no conflict of interest.

References

[1] J. Ni, Y. Sheng, Q. Xiao, Z. Zeng, T. Huang, Stability of partially unstable discrete-time switched positive nonlinear systems with delays, Applied Mathematics and Computation 507 (2025) 129591.

[2] Y. Hou, Y.-J. Liu, S. Tong, Event-triggered fault-compensation-based fuzzy finite-time FTC for MIMO switched nonlinear systems, Applied Mathematics and Computation 496 (2025) 129316.

[3] B. Wang, F. Zou, J. Wu, J. Cheng, A learning-based sliding mode control for switching systems with dead zone, Applied Mathematics and Computation 494 (2025) 129283.

[4] M. Fiacchini, M. Jungers, A. Girard, Stabilization and control Lyapunov functions for language constrained discrete-time switched linear systems, Automatica 93 (2018) 64–74.

[5] J. C. Geromel, P. Colaneri, Stability and stabilization of continuous-time switched linear systems, SIAM Journal on Control and Optimization 45 (5) (2006) 1915–1930.

[6] J. Hespanha, A. Morse, Stability of switched systems with average dwell-time, in: Proceedings of the 38th IEEE Conference on Decision and Control (Cat. No.99CH36304), Vol. 3, 1999, pp. 2655–2660.

[7] L. Vu, D. Chatterjee, D. Liberzon, Input-to-state stability of switched systems and switching adaptive control, Automatica 43 (4) (2007) 639–646.

[8] X. Zhao, L. Zhang, P. Shi, M. Liu, Stability and stabilization of switched linear systems with mode-dependent average dwell time, IEEE Transactions on Automatic Control 57 (7) (2012) 1809–1815.

[9] M.-R. Kong, Y.-W. Wang, Z.-H. Zeng, X.-K. Liu, Adaptive tracking control of switched stochastic non-linear systems with full state constraints: A MDADT switching method, International Journal of Robust and Nonlinear Control 35 (9) (2025) 3763–3777.

[10] W.-H. Wang, Y.-W. Wang, X.-K. Liu, Z.-W. Liu, Quantization-dependent dynamic event-triggered control for networked switched systems under denial-of-service attacks, IEEE Transactions on Systems, Man, and Cybernetics: Systems 54 (6) (2024) 3822–3833.

[11] G. Zong, H. Xie, D. Yang, X. Zhao, Y. Yi, Adaptive fuzzy tracking control for switched nonlinear systems under FDI attacks and input saturation: A flexible transient performance approach, IEEE Transactions on Cybernetics 54 (12) (2024) 7479–7488.

[12] X.-M. Liu, X.-H. Chang, Adaptive event-triggered tracking control for nonlinear networked systems with dynamic quantization and deception attacks, International Journal of Robust and Nonlinear Control 34 (12) (2024) 8311–8333.

[13] J. Yang, X. Zhao, X. Bu, W. Qian, Stabilization of switched linear systems via admissible edge-dependent switching signals, Nonlinear Analysis: Hybrid Systems 29 (2018) 100–109.

[14] C. Yang, S. Zhong, X. Liu, W. Dai, L. Zhou, Adaptive composite suboptimal control for linear singularly perturbed systems with unknown slow dynamics, International Journal of Robust and Nonlinear Control 30 (7) (2020) 2625–2643.

[15] Y. Lei, Y.-W. Wang, X.-K. Liu, W. Yang, Zeno-free event-triggered fixed-time control of two-time-scale systems by chang transformation and backstepping design, Nonlinear Dynamics 111 (7) (2023) 6379–6393.

[16] Y. Lei, T. Hua, Y.-W. Wang, J. H. Park, Robust output regulation of singularly perturbed systems by event-triggered output feedback, IEEE Transactions on Systems, Man, and Cybernetics: Systems 54 (4) (2024) 2104–2113.

[17] M. Long, H. Su, B. Liu, Second-order controllability of two-time-scale multi-agent systems, Applied Mathematics and Computation 343 (2019) 299–313.

[18] T. Hua, J.-W. Xiao, X.-K. Liu, Y. Lei, Y.-W. Wang, Event-triggered sub-optimal control for two-time-scale systems with unknown dynamics, Nonlinear Dynamics 111 (3) (2023) 2487–2500.

[19] W. Yang, X.-K. Liu, Y.-W. Wang, Z.-W. Liu, J.-W. Xiao, Secure stabilization of singularly perturbed switched systems under deception attacks, Nonlinear Dynamics 108 (1) (2022) 683–695.

[20] M. Zhang, Y. Sun, X. Yang, J. H. Park, Secure state estimation of singularly perturbed switched systems with output deception attack via discretized LKF approach, IEEE Transactions on Circuits and Systems II: Express Briefs 71 (2) (2024) 792–796.

[21] G. Zong, C. Zhang, W. Qi, C. K. Ahn, X. Xie, Finite-time control synthesis for discrete fuzzy switched singularly perturbed systems, IEEE Transactions on Circuits and Systems II: Express Briefs 70 (3) (2023) 1109–1113.

[22] X. Ma, Q. Wang, L. Zhou, C. Yang, Controller design and analysis for singularly perturbed switched systems with actuator saturation, International Journal of Robust and Nonlinear Control 26 (15) (2016) 3404–3420.

[23] Q. Wang, L. Zhou, X. Ma, C. Yang, Disturbance rejection of singularly perturbed switched systems subject to actuator saturation, International Journal of Robust and Nonlinear Control 28 (6) (2018) 2231–2248.

[24] Y.-J. Liu, S. Lu, D. Li, S. Tong, Adaptive controller design-based ABLF for a class of nonlinear time-varying state constraint systems, IEEE Transactions on Systems, Man, and Cybernetics: Systems 47 (7) (2017) 1546–1553.

[25] Z. Zhao, W. He, C. Mu, T. Zou, K.-S. Hong, H.-X. Li, Reinforcement learning control for a 2-DOF helicopter with state constraints: Theory and experiments, IEEE Transactions on Automation Science and Engineering 21 (1) (2024) 157–167.

[26] J. Wang, J. Ma, H. Pan, W. Sun, Event-triggered adaptive saturated fault-tolerant control for unknown nonlinear systems with full state constraints, IEEE Transactions on Automation Science and Engineering 21 (2) (2024) 1837–1849.

[27] A. Bemporad, Model predictive control design: New trends and tools, in: Proceedings of the 45th IEEE Conference on Decision and Control, IEEE, 2006, pp. 6678–6683.

[28] J. Nubert, J. Köhler, V. Berenz, F. Allgöwer, S. Trimpe, Safe and fast tracking on a robot manipulator: Robust mpc and neural network control, IEEE Robotics and Automation Letters 5 (2) (2020) 3050–3057.

[29] A. Bemporad, A piecewise linar regression and classification algorithm with application to learning and model predictive control of hybrid systems, IEEE Transactions on Automatic Control 68 (6) (2023) 3194–3209.

[30] N. Chauffert, P. Ciuciu, J. Kahn, P. Weiss, A projection method on measures sets, Constructive Approximation 45 (2017) 83–111.

[31] W. Heemels, M. K. Camlibel, M. F. Heertjes, Oblique projected dynamical systems and incremental stability under state constraints, IEEE Control Systems Letters 4 (4) (2020) 1060–1065.

[32] K. Zhao, Y. Song, Removing the feasibility conditions imposed on tracking control designs for state-constrained strict-feedback systems, IEEE Transactions on Automatic Control 64 (3) (2019) 1265–1272.

[33] L. Zhu, D. Huang, X. Li, Q. Wang, Cooperative operation control of virtual coupling high-speed trains with input saturation and full-state constraints, IEEE Transactions on Automation Science and Engineering 21 (3) (2024) 3497–3510.

[34] Y. Jiang, F. Wang, Z. Liu, Z. Chen, Composite learning adaptive tracking control for full-state constrained multiagent systems without using the feasibility condition, IEEE Transactions on Neural Networks and Learning Systems 35 (2) (2022) 2460–2472.

[35] H. Wang, C. Yang, X. Liu, L. Zhou, Neural-network-based adaptive control of uncertain MIMO singularly perturbed systems with full-state constraints, IEEE Transactions on Neural Networks and Learning Systems 34 (7) (2023) 3764–3774.

[36] F.-M. Huang, C. Liu, Quantized fuzzy guaranteed cost control for electric vehicle with uncertain parameters, Applied Mathematics and Computation 523 (2026) 130019.

[37] X. Jin, Adaptive fixed-time control for MIMO nonlinear systems with asymmetric output constraints using universal barrier functions, IEEE Transactions on Automatic Control 64 (7) (2019) 3046–3053.

[38] C. Wang, Y. Lin, Multivariable adaptive backstepping control: a norm estimation approach, IEEE Transactions on Automatic Control 57 (4) (2012) 989–995.

[39] M. A. Müller, P. Martius, F. Allgöwer, Model predictive control of switched nonlinear systems under average dwell-time, Journal of Process Control 22 (9) (2012) 1702–1710.